PERFORMANCE OF CAPACITIVE CANTILEVER SENSOR FOR PORTABLE HEAVY METAL ION DETECTOR

TAN YOONG TENG

UNIVERSITI TEKNIKAL MALAYSIA MELAKA

PERFORMANCE OF CAPACITIVE CANTILEVER SENSOR FOR PORTABLE HEAVY METAL ION DETECTOR

TAN YOONG TENG

This report is submitted in partial fulfilment of the requirements for the degree of Bachelor of Electronic Engineering with Honours

Faculty of Electronics and Computer Technology and Engineering
Universiti Teknikal Malaysia Melaka

2024

DECLARATION

I declare that this report entitled "Performance of capacitive cantilever sensor for portable heavy metal ion detector" is the result of my own work except for quotes as cited in the references.

Signature : ....

Author : TAN YOONG TENG

Date : ....24/06/2024...............

APPROVAL

I hereby declare that I have read this thesis, and, in my opinion, this thesis is sufficient in terms of scope and quality for the award of Bachelor of Electronic Engineering with Honours

Signature : ....

Supervisor Name : Ts. Dr. Norihan Abdul Hamid
Pensyarah Kanan
Fak. Tek. & Kej. Elektronik & Komputer
(FTKEK) Universiti Teknikal Malaysia Melaka
(UTeM) Hang Tuah Jaya, Melaka

Date : 24/06/2024

DEDICATION

The completion of this thesis would not have been possible without the help and guidance of many individuals. Firstly, I am profoundly grateful to my supervisor, Dr. Norihan Binti Abdul Hamid, for her unwavering support, motivation, enthusiasm, and extensive knowledge. Her assistance and dedicated involvement in every phase of this project were crucial for its completion. I could not have asked for a better supervisor for my final year project. Additionally, I would like to extend my heartfelt thanks to my lecturers and the panels whose guidance, support, and encouragement have been invaluable throughout this project. Their ideas and recommendations during the project presentations significantly improved my work. I also wish to express my deepest gratitude to my beloved parents and friends, especially Khor Kelly, for their relentless support and spiritual encouragement throughout my PSM journey. This thesis stands as a testament to their unconditional love and encouragement. Finally, I am thankful to Universiti Teknikal Malaysia Melaka for providing me with the opportunity to pursue my studies and successfully complete my final year project.

ABSTRACT

Heavy-metal ions (HMIs) are environmental pollutants that readily react with biological matter to cause serious toxicological and carcinogenic effects on body systems and vital organs. Access to safe drinking water remains a pressing global concern, affecting one in three people worldwide, while the presence of heavy metal ions (HMIs) in water sources poses a severe health threat even at trace levels. The challenge lies in efficiently detecting these pollutants on-site, as existing methods often lack the necessary efficiency, portability, and affordability, hampering early pollution warnings, regulatory enforcement, and decentralized water monitoring efforts. Thus, this project is to analyze the performance of the microcantilever beam by observing the maximum deflection with respect to force applied where the force acts as the mass of HMIs detected. COMSOL 5.5 software was first implemented to determine the best sensing materials that will result in maximum deflection based on different properties such as Young Modulus and Poisson Ratio which related with Stoney's formula. ANSYS software was used for conducting a Finite Element Analysis using 4 different Stress Concentration Region which are Rectangular, Square, Circular and Triangular. The performance of the beam was analyzed and compared with and without the presence of SCR. The relationship of the dimension of stress concentration region was determined. At the end of this project, a suitable dimension of cantilever beam was proposed with best sensing material determined along with the stress concentration region that result in maximum deflection. Both results obtained from 2 software were compared with previous studies.

ABSTRAK

Ion logam berat (HMI) ialah bahan pencemar alam sekitar yang mudah bertindak balas dengan bahan biologi untuk menyebabkan kesan toksikologi dan karsinogenik yang serius pada sistem badan dan organ penting. Akses kepada air minuman yang selamat kekal menjadi kebimbangan global yang mendesak, yang menjejaskan satu daripada tiga orang di seluruh dunia, manakala kehadiran ion logam berat (HMI) dalam sumber air menimbulkan ancaman kesihatan yang teruk walaupun pada tahap surih. Cabarannya terletak pada pengesanan bahan pencemar ini dengan cekap di tapak, kerana kaedah sedia ada sering kekurangan kecekapan, mudah alih dan kemampuan yang diperlukan, menghalang amaran pencemaran awal, penguatkuasaan kawal selia dan usaha pemantauan air terpencar. Oleh itu, projek ini adalah untuk menganalisis prestasi rasuk mikrocantilever dengan memerhatikan pesongan maksimum berkenaan dengan daya yang dikenakan di mana daya bertindak sebagai jisim HMI yang dikesan. Perisian COMSOL 5.5 mula dilaksanakan untuk menentukan bahan penderiaan terbaik yang akan menghasilkan pesongan maksimum berdasarkan sifat yang berbeza seperti Modulus Muda dan Nisbah Poisson yang berkaitan dengan formula Stoney. Perisian ANSYS digunakan untuk menjalankan Analisis Elemen Terhingga menggunakan 4 Wilayah Kepekatan Tekanan yang berbeza iaitu Segi Empat, Segi

Empat, Pekeliling dan Segi Tiga. Prestasi rasuk dianalisis dan dibandingkan dengan dan tanpa kehadiran SCR. Hubungan dimensi kawasan kepekatan tegasan ditentukan. Pada akhir projek ini, dimensi rasuk julur yang sesuai telah dicadangkan dengan bahan penderiaan terbaik ditentukan bersama dengan kawasan kepekatan tegasan yang mengakibatkan pesongan maksimum. Kedua-dua keputusan yang diperoleh daripada 2 perisian dibandingkan dengan kajian lepas.

ACKNOWLEDGEMENTS

First and foremost, I would like to express my gratitude to God for enabling me to complete this project successfully. I would also like to extend my heartfelt thanks to my supervisor, Dr. Norihan Binti Abdul Hamid, whose invaluable guidance and instructions were crucial in making this project a complete success. Her suggestions played a major role in the project's completion.

I am deeply thankful to my parents and friends for their valuable suggestions and guidance, which were helpful during various phases of this project.

Finally, I would like to express my appreciation to Universiti Teknikal Malaysia Melaka for providing me with the opportunity to pursue my studies and successfully complete my final year project.

TABLE OF CONTENTS

LIST OF FIGURES

LIST OF TABLES

LIST OF SYMBOLS

F	:	Force
δ	:	Total deflection of the beam
E	:	Young Modulus
w	:	Width of the beam
L	:	Length of the beam
t	:	Thickness of the beam
v	:	Poisson ratio
k	:	Spring constant
σ	:	Density
μ	:	Micro unit
N	:	Newton
Pa	:	Pascal

LIST OF ABBREVIATIONS

MEMS	:	Micro-electromechanical system
FEA	:	Finite Element Analysis
SCR	:	Stress Concentration Region
WHO	:	World Health Organization
HMI	:	Heavy Metal Ion
EPA	:	Environmental Protection Agency
Cu	:	Copper
Pb	:	Lead
Cd	:	Cadmium
Hg	:	Mercury
As	:	Arsenic
SPOT	:	Superhydrophobic Concentrator
SAM	:	Self-assembled monolayers
CS	:	Chitosan
GO	:	Graphene Oxide
SPR	:	Surface plasmon resonance
AC	:	Alternating Current
ASV	:	Anodic Stripping Voltammetry
SWV	:	Square Wave Voltammetry

ARM	:	Advanced RISC Machines
EIS	:	Electrochemical impedance spectroscopy
µISE	:	Miniature ion-selective electrode
C4D	:	Capacitive Coupled Non-Contact Conductivity Selection
DNA	:	Deoxyribonucleic acid
FEP	:	Finite Element Program
CAD	:	Computer-aided design
CFD	:	Computational Fluid Dynamics
DOF	:	Degree of Freedom

LIST OF APPENDICES

CHAPTER 1

INTRODUCTION

This chapter includes the background of the project which includes the project overview, problem statement, objectives, and scope of the project.

1.1 Research Background

Heavy metal ions (HMIs) represent one of the major pollutants inside the water nowadays as it has caused some serious health problems after long periods of consuming the water samples. Environmental issues causing some enormous effect on human life globally which water contamination is proven to be very hazardous according to the World Health Organization (WHO) and others related health organizations. This serious issue requires an immediate solution to resolve it and propose a method of preventing such cases happening in future time.

There are quite a few methods that can be implemented on the role of heavy metal ion detection including atomic absorption spectroscopy method, inductively coupled plasma, and inductively coupled plasma mass spectrometry where these techniques facing some advantages such as having low detection limits and multiple of ions can be measured simultaneously by using these techniques [1]. These methods required both optical and electrochemical sensors which have characteristics of highly sensitive and selective compared to other sensors. The working principle is different for both sensors as they implement the changes in optical and electrical signal about the target molecule [2].

Recently, micro-electromechanical (MEMs) based sensors are widely used in various industries, civil, defense applications and can present serious medical, environmental and explosion dangers. The working of this sensor is by converting the changes whenever it acts on the sensor into electrical responses and so this capability plays a vital role on different sensing platform by implementing a MEMs based sensor with precise detection of the response and hence conduct amplification and measuring process. Detection of heavy metal ions in water using MEMS (Micro-Electro-Mechanical Systems) based sensors is a cutting-edge field with substantial implications for environmental monitoring and public health. MEMS technology, renowned for miniaturization and precision, offers a promising avenue for developing highly sensitive and portable sensors capable of detecting trace amounts of heavy metals in water.

MEMS-based sensors for heavy metal ion detection typically employ various innovative designs. For instance, microcantilevers, with their ability to bend in response to minute forces, can be functionalized with specific receptors that selectively bind to target heavy metal ions [3]. This binding causes mechanical deflection, which can be translated into an electrical signal, enabling the quantification of metal ion concentrations. Nanostructured materials play an essential role in enhancing the sensitivity of these sensors. Utilizing nanomaterials, such as nanowires or nanoparticles, on the sensor's surface amplifies the surface area available for interactions with heavy metal ions. This increases the chances of ion capture, significantly improving the sensor's detection limits.

Hence, the MEMs based microcantilever has been propose in this report to responsible for using it in heavy metal ion detection and according to statistic, it has been proven as an outstanding platform for extremely sensitive chemical and biological sensors. Microcantilever has gained a lot of popularity in the past decade due to its high sensitivity, selectivity, ease for fabrication and on-chip circuit flexibility [4]. There are no extra external detection devices required by implementing this microcantilever sensor and it has become interesting since it is easy to calibrate, can be quickly included into an integrated electromechanical system.

Cantilever beam as a sensing element is becoming more general as it certainly represents the most favorable devices that bend when a pressure is applied on one of the ends then results in an oscillation like a spring. In this paper, the design of a MEMs based microcantilever using COMSOL Multiphysics will be discussed. The behavior of the sensor at different pressure and the displacement change will be determined. First, the dimensions of the cantilever should be considered to provide the best sensitivity by altering the length, width, and height of the cantilever beams.

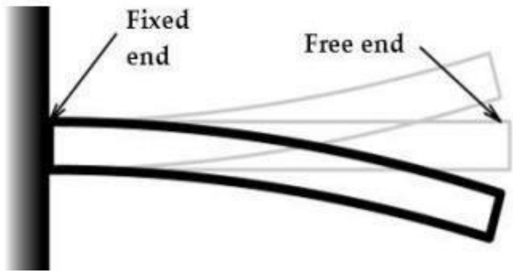

Figure 1.1: Idea of a cantilever beam

An optimum dimension can be determined by analyzing the displacement change with different force applied on one end of the cantilever. After the determination of the best dimension of the cantilever by defining the types of material used, the geometry shapes, fixed constraint at one side of the cantilever to ensure that it will not rotate for both side and it is free for another side to bend.

After that, ANSYS software will be implemented using the dimension of the cantilever beam that has been determined to conduct a Finite element analysis (FEA). Different types of Stress Concentration Region (SCR) are used to compare the deflection with respect to force and the assumption of variation in Heavy Metal Ion is ensured to fulfill the standard of the World Health Organization (WHO) data and hence the performance of the cantilever is analyzed with different SCR.

The most recent study on microcantilevers uses them as a platform for applications involving gas sensing. Coatings of chemically sensitive materials are applied to microcantilevers, which are utilised to detect the presence of specific particles or analytes. This substance will offer a high level of specificity when it comes to identifying individual particles or analytes in a sample. This micro cantilever deflection happens when a particular analyte mass is adsorbed on its surface in a particular way. When a force is applied, it would consequently result in a deflection at the free end.

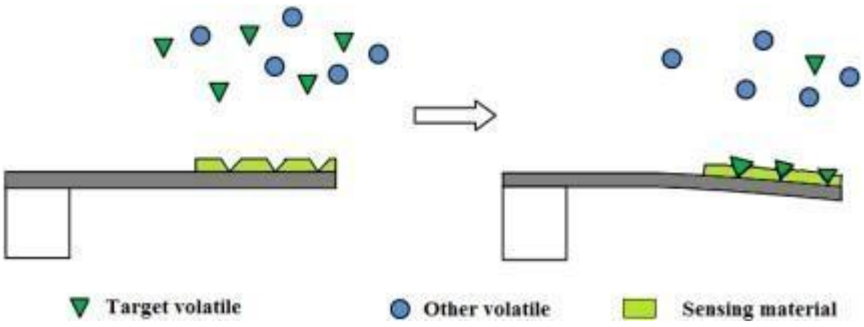

Figure 1.2: General structure of a microcantilever gas sensing application

Microcantilevers use their elasticity or flexibility to sense changes in response to different stimuli, which can be measured. The term "mechanical stress" describes the cantilever's response, which modifies the cantilever's electrical or mechanical characteristics. The resistivity, angular deflection, and natural resonant frequency of the microcantilever are the most measured parameters to identify these modifications. By functionalizing one surface of the cantilever with a particular detector layer, this approach can act as a sensing mechanism and directly quantify changes in surface tension.

To obtain optimal design parameters for specific applications and predict cantilever performance, ANSYS Workbench 2024 R1 software was used. The small size of the microcantilever offers significant advantages in terms of absolute device sensitivity. This setup allows for precise measurement of the deflection at the end of the cantilever.

1.2 Problem statement

Nowadays, environmental pollutants known as heavy metal ions (HMIs) can react quickly with biological material to produce harmful toxicological and carcinogenic effects on our bodies and vital organs. The ecosystem's buildup of non-biodegradable heavy metals and the growing pollution caused by humans resulting from population as well as manufacturing worsen these risks to health [5]. Taking example from Flint water crisis during which lead leached into the water distribution system because of the flow of corrosive river water in aging pipes. The lead concentration was then measured after 10 months, and it is found that the value was 1000-fold higher than the EPA's permissible limit. Therefore, it is essential to carry out easy-to-operate routine for HMI monitoring, especially in portable water so an ultrasensitive detection of HMIs is thus an important defense against heavy-metal poisoning because it enables early pollution warning and efficient regulatory enforcement. Addressing that, the main aim of this project is to propose portable and cost-effective MEMs based heavy metal ion sensors to detect and monitor the metal ions value.

1.3 Objectives

The objectives of the project are as follows:

a) To design a MEMs based capacitive microcantilever beam and analyze suitable sensing material using COMSOL software.

b) To simulate a microcantilever beam HMI sensor and analyze the maximum deflection with variation force that act as the mass of HMI detected.

c) To evaluate the performance of the microcantilever beam using 4 different Stress Concentration Region approaches and compare its sensitivity in ANSYS software.

1.4 Scope of Research

1. Study on the characteristics of different types of Heavy Metal Ion inside water (Copper (Cu), Lead (Pb), Cadmium (Cd), Mercury (Hg) and Arsenic (As)) that harm and cause serious toxicological and carcinogenic effects on body systems and vital organs.
2. Design, simulate and analyze a portable, sensitive, and cost-effective MEMs based heavy metal ion sensor using Finite Element Analysis (FEA) in COMSOL software. Optimize the design based on capacitance variation with respect to dimension, length, and thickness of cantilever beam.
3. Conducting Finite element analysis (FEA) of different Polysilicon microcantilever shapes in two different Stress Concentration Region (SCR) using ANSYS software. Analyze the sensitivity of the microcantilever beam using different SCR by comparing the deflection with respect to force.

CHAPTER 2

BACKGROUND STUDY

This chapter covers the background of heavy metal ion detection, different techniques used on conducting the detection along with its advantages and disadvantages. Furthermore, the types of analysis of the cantilever beam inside COMSOL Multiphysics software also have been highlighted this topic.

2.1 Review of the techniques used on HMIs detection

Research done by Tao Hu (2020) proposed that optical and electrochemical sensing methods are promising for portable heavy metal ion sensing due to their high sensitivity, selectivity, and economy. Portable optical heavy metal ion sensors based on fluorescence, colorimetric, portable surface Raman enhancement, and plasmon resonance have been developed, while electrochemical sensors based on electrical parameter analysis principles such as potentiometry, amperometry, and voltammetry have also been reported. The author proposed for the future research to focus on developing new sensing materials and signal amplification strategies to improve the sensitivity and selectivity of the sensors, developing miniaturized and integrated sensor devices that are easy to use and operate, and developing portable sensor devices that can be used in a wider range of environmental conditions. [6]

Satyam Srivastava (2020) states that existing HMI detection methods are often complex, expensive, and time-consuming, limiting their applicability for in situ and real time monitoring. It presents an ultra-portable, rapid, cost-effective, and easy-to-use system for onsite heavy metal concentration measurement in drinking water samples. It combines off-the-shelf chemical kits for heavy metal detection with a developed spectrometer-based readout for concentration prediction, quality judgment, and automatic data collection. The system was trained and tested with real-world water samples, demonstrating excellent accuracy in predicting heavy metal concentrations. [7]

Moreover, the portable HMI sensing is critical research due to toxicity and ubiquity and a paper done by Yi Cui (2021) has introduces a portable Superhydrophobic concentrator sensor (SPOT), for the concurrent quantification of five different heavy metal ions (HMIs) down to the sub-nanomolar level. SPOT is based on a colorimetric reaction between the HMIs and a sulfiding agent on a superhydrophobic surface. The superhydrophobic surface concentrates the analytes for sensitive visual detection. SPOT can be made portable by being integrated with a smartphone application, enabling rapid and cost-effective HMI detection on site. The time taken for analysis is short with quite a low-cost but indeed need the help of an android application system for analyzing purpose. [8]

Binesh Unnikrishnan (2021) proposed a new and promising approach using a metal nanozyme based assays. Metal nanozyme-based assays work by detecting the changes in the catalytic activity of the nanozyme when it binds to the metal ion of interest. These changes can be measured using a variety of techniques, such as UV- vis absorption spectroscopy and fluorescence spectroscopy. It shows high sensitivity for variety of heavy metal ions, including lead, cadmium, mercury, and arsenic. [9]

Besides that, microfluidic platform also played an important role and acted as a new technology for HMIs detection with its low cost, portable and rapid time characteristics. According to Dinesh Rotake (2018), these platforms typically use microcantilever beams surface modified with different proteins to selectively detect HMIs. The sensitivity of the platforms can be improved by using different shapes, stress concentration regions (SCRs), and dimensions for the microcantilever beams. It also uses a capacitive microcantilever beam to detect the changes in pressure due to HMIs. [10]

Microcantilevers functionalized with metal-binding protein “AgNt84-6” are demonstrated as good sensors for the detection of heavy metal ions like Hg^{2+} and Zn^{2+} by [11]. SAMs (self-assembled monolayer’s) modified microcantilevers used for detection of Ca^{2+} ions are presented in [12]. Arrays of microcantilever sensors encapsulated in fluidic wells and fluidic channel are discussed in [13] and [14], respectively. A Chitosan (CS)-graphene oxide (GO) Surface Plasmon resonance (SPR) sensor is explained in [15] while, simple microcantilever beam based detection is given in [16-18]. Since all these methods use optical readout, require heavy setup and costly lab equipment. The analysis of different shapes and stress concentration region (SCR) to improve the sensitivity of microcantilever beam has been very well explained in [19-22] but for microfluidic application these dimensions are not suitable and need to be investigated.

2.1 Technique used on measured accuracy of microcantilever beam.

In this part, the technique that we used to analyze the performance of the cantilever beam will be discussed. For chemical performance, the cantilever beams are coated directly by samples or sensor layers and then exposed to analyte vapors [24]. The way on measuring the performance of the cantilever is divided into static way and dynamic way where for static way mainly depends on the shift in bending whereas for dynamic way basically is by monitoring the resonant frequency. So, in this session various ways on measured the microcantilever beam including optical reflection, piezoresistive, capacitance and piezoelectric methods which are the most common methods with high accuracy. The advantage of using these techniques is that we can measure both frequency and bending in a single measurement. [25]

2.1.1 Optical Beam Deflection

In this technique basically it is based on the deflection of an optical beam where the beam will irradiate the surface of the rail and is reflected at angles that depend onthe orientation of the surface at the point of measurement, which is perturbed by the passage of the acoustic wave. The optical beam deflection represents the easiest method to measure the deflection of a cantilever beam. A laser diode will focus on the free end of the cantilever where the other end had been fixed to monitor the displacement of bending. The reflected beam will be examined by implementing a position sensing detector and the number of displacements can be up to 0.1nm by using this technique [23].

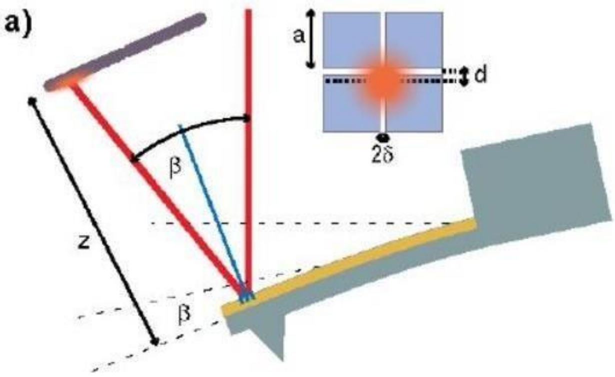

Figure 2.1: Principle of classical optical beam deflection

2.1.2 Piezoelectric technique

This technique leverages the properties of piezoelectric materials. The microcantilever beam's surface is coated with a thin layer of piezoelectric material, which generates a transient charge when the beam moves [26]. When the environmental excitation frequency matches the natural frequency of the piezoelectric cantilever beam, the beam resonates, resulting in maximum amplitude and output voltage. Initially, the excitation frequency and the environmental force are determined. Then, the relationship between the beam's dimensions and its natural frequency is established using finite element analysis. However, a drawback of this technique is that it requires electrodes to be attached to the piezoelectric film, and it is typically employed in the dynamic mode of the cantilever beam.

2.1.3 Piezoresistance technique

Piezoresistive techniques in microcantilever beam design involve leveraging the piezoresistive effect which represents a change in electrical resistance due to mechanical strain to enhance sensing capabilities. By integrating piezoresistive elements into the microcantilever structure, changes in mechanical stress or strain can be converted into measurable electrical signals, augmenting the sensor's sensitivity and accuracy [27].

The designing of a microcantilever beam with piezoresistance will often dope with semiconductors like silicon or germanium, within or onto the beam structure. As the microcantilever undergoes bending or deflection due to external forces or stimuli, these piezoresistive elements experience strain, altering their electrical resistance. This change in resistance is then measured using appropriate circuitry, converting mechanical deformation into a quantifiable electrical signal.

Deflection can be induced by making changes in the adsorption-induced stress or by thermal stress. The variation in resistance can be measured by using an external dc biased, Wheatstone bridge [3]. The disadvantage of this method is that cantilever should be given with passing current throughout which creates electric noises and thermal drift in micro cantilever deflection.

Piezoresistive cantilever detection is known to have lower resolution compared to optical detection. The piezoresistive effect in silicon is well-documented in literature, showing that the resistance R changes with applied stress, influenced by factors such as crystal orientation, dopant type, and doping concentration. The piezoresistive sensitivity for a resistor with area A_R is expressed as:

$$\frac{\Delta R}{R} = \frac{\int (\rho_L \sigma_L + \rho_T \sigma_T) dA}{A_R} \tag{2.1}$$

where ρ_L is the longitudinal piezoresistive coefficient (for stress parallel to the current flow), ρ_T is the transverse piezoresistive coefficient (for stress perpendicular to the current flow), σ_L is the longitudinal stress, σ_T is the transverse stress, and A_R is the area of the resistor. The integration accounts for the non-uniform stress along the length and width of the resistor and dividing the result by the area gives the average stress in the resistor region. Maximizing stress in the resistor region enhances the piezoresistive sensitivity of the device, improving detection capability while considering resistor noise. From (2.1) can be seen that the piezoresistive sensitivity depends on the stress in the resistor and to increase the sensitivity, it is obviously essential to maximize the stress in resistor to provide higher sensitivity of the device. Moreover, the piezoresistive detection capability will improve by taking in the considerations of the noise that appears inside the resistor.

2.1.4 Capacitance measurement technique

In designing microcantilever beams, capacitance measurement techniques are used to detect and measure displacement of the beam or changes in its position [29]. Capacitive sensing is done through changes in the capacitance due to variations in distance between conducting surfaces, differences that arise upon bending and displacement of a microcantilever.

This method usually required parallel conducting plates or electrodes to the structure to perform capacitance measurement on microcantilevers. When a microcantilever bends or deflects in response to an external force, the distancebetween these two plates changes too. This change alters the capacitance between them also. The beam displacement or deflection is directly proportional to this change in capacitance. The capacitance changes can be quantified by using an alternating current (AC) or high-frequency signal to the capacitive structure and measuring various electrical parameters such as phase shifts of changes in amplitude. These represent variations in capacitance that occur when a microcantilever moves from one position to another under interaction with its surroundings.

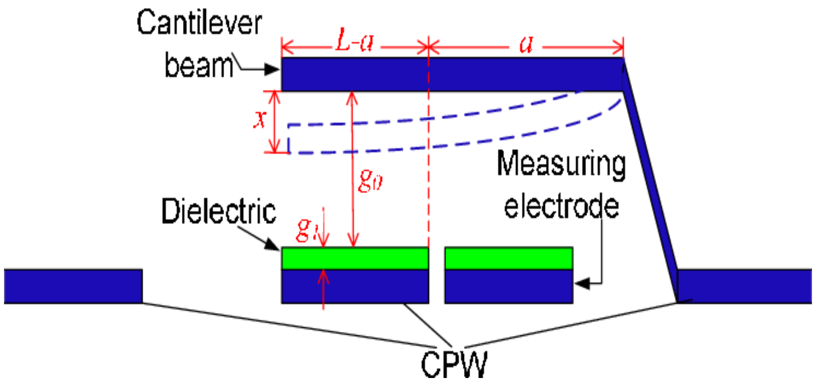

Figure 2.2: Capacitive based cantilever beam

2.2 Electrochemical methods on HMIs detection

Given its high sensitivity and effectiveness, electrochemical detection is considered one of the most effective technologies for detecting heavy metal ions. Using a constant potentiometer to generate a transducer signal and identify potential variations is the basic idea behind electrochemical sensors. Numerous electrical characteristics, including voltage, potential, impedance, conductance, and capacitance, are altered when heavy metal ions are present. Consequently, conductivity measurements, voltammetry, impedance, and potentiometry are the main methods utilised in electrochemical detection.

2.2.1 Voltammetry

Voltammetry is a useful method for detecting heavy metal ions in a range of intricate settings. Anodic Stripping Voltammetry (ASV), with its linear dynamic range, high sensitivity, and broad applicability, is an efficient voltametric technique. To detecting Cd and Pb ions in soil samples, a low-cost electronic circuit has been created. To detect ions in accordance with the ASV principle, concentrations, they affixed screen-printed electrodes on glassy carbon electrodes and connected them to a circuit for electrochemical analysis whereas to make the system portable, a voltage converter was used to implement the control circuit of the electrochemical laboratory [30].

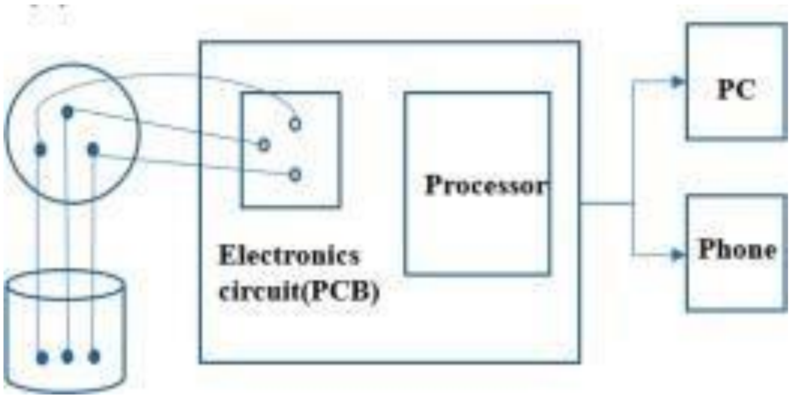

Figure 2.3: Electrochemical sensor for cadmium and copper detection

Another common application for square wave voltammetry (SWV) is the portable detection of copper ions in water. A miniature detecting circuit module and a specially designed electrochemical electrode make up the sensor hardware. A multi-channel constant potential metre may be precisely controlled by the detecting circuit module using an ARM chip, which also makes it easier to acquire weak current signals.

ARM chips are renowned for their computational power and energy efficiency, making them ideal for controlling sensitive measurement devices like constant potential meters used in sensing applications. The ARM chip's capabilities ensure accurate and stable control of multiple channels, essential for reliable detection of signals from various sources or sensors, such as those in microcantilever-based systems for detecting small mechanical changes or biochemical interactions.

2.2.2 Impedance method

The most widely used impedance measurement techniques for determining the concentration of analytes in aqueous solutions include electrochemical impedance spectroscopy (EIS) and alternating current voltammetry. This method relies on measuring changes in impedance, which is the opposition offered by the solution to the flow of an alternating current (AC), as heavy metal ions interact with an electrode surface [31].

The process involves a working electrode immersed in the solution containing the heavy metal ions of interest. When a small AC voltage is applied to the electrode, it generates an AC current that interacts with the ions at the electrode-electrolyte interface. The impedance of this system which is affected by the presence and concentration of heavy metal ions will alter due to changes in charge transfer resistance, double-layer capacitance, or other electrochemical processes occurring at the electrode surface.

In the context of heavy metal ion detection, impedance-based electrochemical sensors can offer advantages such as high sensitivity, rapid response, and the ability to detect multiple analytes simultaneously. These sensors can be designed withspecific electrode materials or surface modifications to enhance selectivity towards heavy metal ions, making them valuable tools for environmental monitoring, water quality assessment, or industrial safety applications.

2.2.3 Potentiometric Method

The method of potentiometry allows for the precise and selective measurement of heavy metal ions in water by focusing on zero-current electric potential. It involves using specific electrodes to analyze ions in a solution. A miniature ion-selective electrode array (µISE) that integrated multiple electrodes onto a single chip, enabling the simultaneous detection of various heavy metal ions. This micro-sized array, created through microfabrication techniques, demonstrated remarkable sensitivity, stability, and rapid response times [32].

The potential between the Ag/AgCl reference electrode and the corresponding µISE electrode was measured using a digital multimeter. As per the Nernst effect principle, while the reference electrode's potential remained constant, the µISE electrode's potential changed with the detected ions' concentrations. The achieved detection limits for Pb2+, Cd2+, and Hg2+ were notably low, reaching 1, 3, and 1 part per billion (ppb), respectively. These findings highlight the potential of this method for accurately assessing drinking water quality by detecting hazardous heavy metal ions within safe limits.

2.2.4 Electrical Conductivity Method

Since conductivity testing has such high sensitivity and selectivity, it has become a popular technique for metal detection. Capacitively coupled non-contact conductivity detection (C4D) is one of these techniques that stands out due to its ease of use, robustness, and defence against electrode contamination. Heavy metal separation and sensitive detection are made possible by the CE-C4D microchip system, which combines capacitively coupled non-contact conductivity detection with capillary electrophoresis.

The development of an integrated lock-in amplifier-based circuit for non-contact conductivity determination of various heavy metals within a rapid timeframe of 100 seconds. This method involved applying a sinusoidal excitation signal to one electrode and measuring the resulting current at another electrode then the current was converted to a voltage and processed through a phase shifter to compensate for signal phase shifts. LabVIEW software was utilized for data acquisition.

The electrophoresis program employed high-voltage modules for injection and separation, using specific voltage parameters for each stage. The achieved detection limits for the tested heavy metals ranged from 0.7 to 5.4 µM. Additionally, a portable device incorporating a polymer microchip system, non-contact conductivity detector, data acquisition system, and user interface was developed. This device enabled on-site detection of metal ions in water samples with a detection limit of 5 µM.

2.2.5 MEMS and Finite Element Analysis

MEMS devices make use of nanofabrication techniques associated with the technology of microelectronics fabrication. This calls for a number of expensive and high-tech procedures, including doping and ultraviolet lithography. Finite element analysis (FEA) is used to characterise the behaviour of MEMS structures during vibration testing, water flow, and DNA binding because manufacture is an expensive process. Early problem detection during the design cycle is made possible by FEA software, which helps MEMS designers cut down on time to market by preventing expensive problems before moving on to fabrication or production. MEMS devices are examined for package stack-up, collision avoidance/detection, functional operation, and design intent throughout the design cycle. By scaling down to sub-micron and angstrom-level characteristics, FEA helps designers develop smaller devices, leading to the development of nano sensors and actuators. For MEMS-based sensing apparatuses that comprise assemblies of several parts and packaging, FEA helps determine collision and contact surfaces.

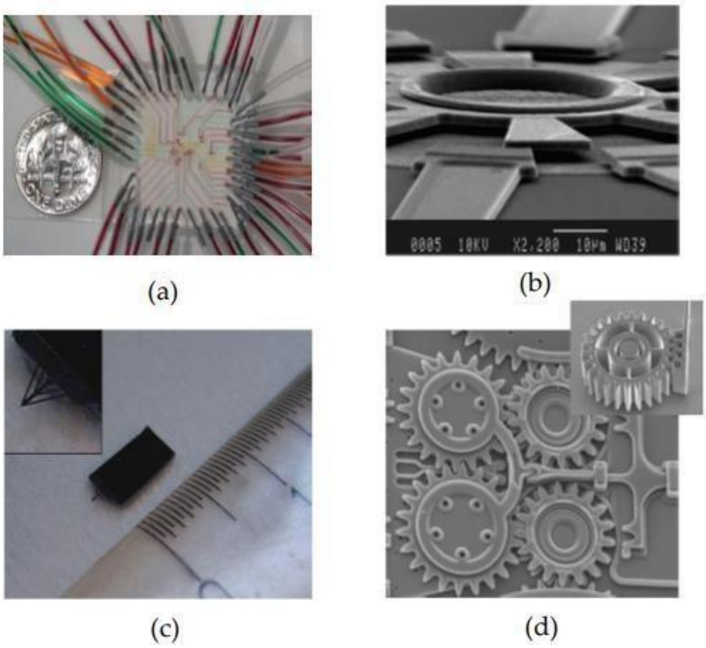

Figure 2.4: Example of MEMS devices

Many FE programmes, like as ANSYS, Solidworks, and Abaqus, are available on the market and have been used to evaluate MEMS devices. In addition, there are specialised MEMS FE programmes like CoventorWare and IntelliCAD that work with the fabrication process of MEMS devices. The modelling and fabrication files were integrated in both programmes, allowing for the transfer of the fabrication equipment. The design modelling file or attachment will serve as the basis for the fabrication. This will assist the MEMS designers in both the analysis and optimisation of the design of the MEMS device as well as its manufacturing viability. Researchers create new designs because of the flexibility in producing many design variations that cover a wide variety of needs, from die-mounted to package assembly to device efficiencies of combinations and this will lead the researchers on developing new device without any fabrication or prototype cost.

2.2.6 MEMS based cantilever sensor and Finite Element Analysis

Brugger et al. (1999) and Thundat et al. (1995) have highlighted that cantilever-based sensors are among the simplest MEMS devices, offering significant potential for developing innovative physical, chemical, and biological sensors. These devices are highly versatile and have been applied in various fields, including accelerometers and chemical sensors [32].

MEMS cantilever sensors fundamentally rely on the mechanical deformation of their structures, specifically the deflection of a membrane or beam structure. When a cantilever is subjected to a load, its stressed elements deform, causing the cantilever to bend. This deformation changes the shape of the structure, displacing points along it. Deflection occurs when a disturbance or load is applied to the free end of the cantilever or along its surface. Typically, the disturbance or load is a force or mass attached to the cantilever, resulting in its bending. Figure 2.5 below illustrates the working principle of MEMS cantilever deflection.

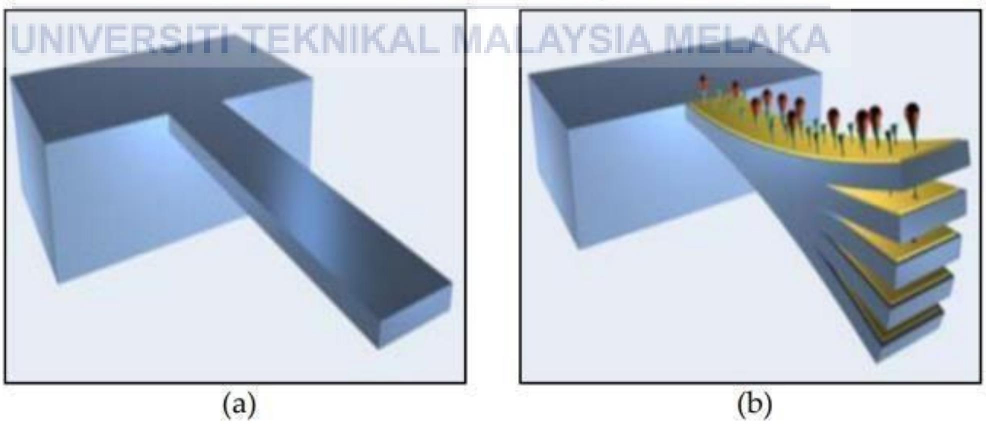

Figure 2.5: MEMS Cantilever sensor with and without binding mass

Bending is the name given to the deformation that occurs when the MEMS cantilever deflects. As illustrated in Figure 2.5, externally applied loads that induce bending will generate reactions at the free end, such as displacement or deflection. Equation (2.2) can be used to determine the maximum deflection during force applied for a beam with a constant cross section. The cantilever deflection diagram with one fixed end and one free end and applied force/mass is shown in Figure 2.6.

$$\delta_{max} = \frac{Fl^3}{3EI} \tag{2.2}$$

Where δ_{max} represent the maximum deflection, F represent the force applied, l is the cantilever length, E is the Young’s modulus of the material that had been implemented in cantilever design and finally I represent the moment inertia for the cantilever.

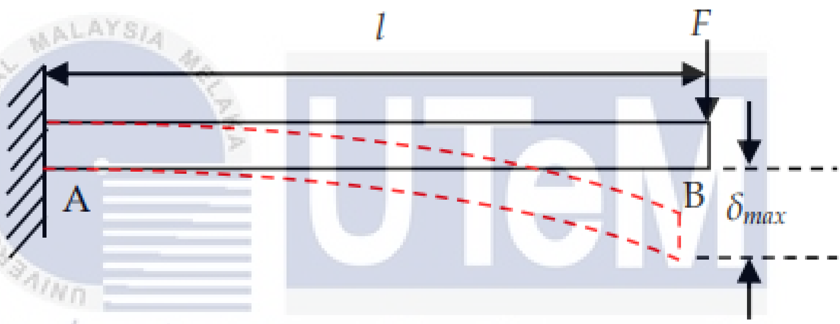

Figure 2.6: Normal schematic for cantilever deflection

Besides that, not only the deflection of the cantilever beam should be considered during a load placed on it but also few stresses will be sensed by the cantilever sensor that occurred during deflection. There are 2 common stresses that will occur during deflection of the cantilever which are tensile stress and compressive stress. These stresses will act in different directions of the cantilever where the tensile stress occurs at the top of the cantilever and compression acts at the bottom of the cantilever. Figure 2.7 below shows the illustration of the stresses that act on the beam in different directions.

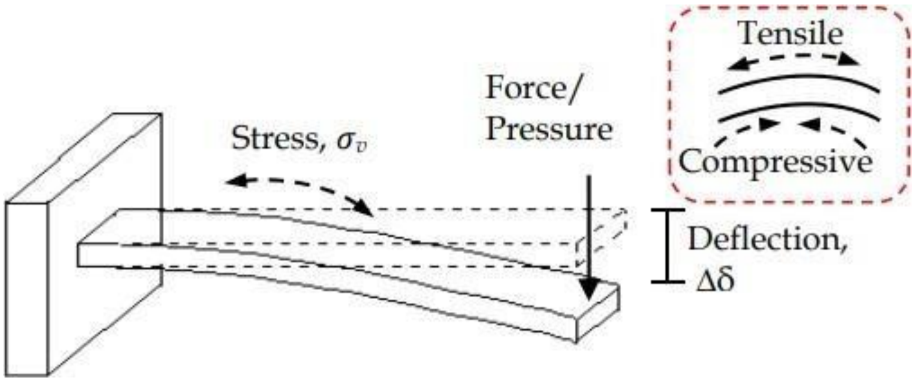

Figure 2.7: Stress distribution when force applied

Another equation can be implemented to calculate the maximum stress for a constant cross section beam.

$$\delta_{max} = \frac{6Fl}{bh^2} \tag{2.3}$$

Where M, moment = F, force multiply by the cantilever length l, δ_{max} represent the maximum stress, b is the width of the cantilever and h represent the height of cantilever.

2.3 Summary and significant result of portable heavy metal ion sensor design

Numerous types of research on the design of a portable heavy metal ion sensor are studied and the findings of the studies are tabulated and discussed. Table 2.1 shows the significant result of the findings of the design of a portable heavy metal ion detector using different kinds of sensors.

Table 2.1: Significant result of portable heavy metal ion detector design.

Author	Title	Finding	Method Used	Limitation	Source	Cost
Dinesh Rotake, A.D. Darji (2018)	Heavy Metal Ion Detection in Water using MEMS Based Sensor	Develop a microfluidic detection platform using capacitive microcantilever beam fabricated by using MEMS technology.	- Microfluidic platform with microcantilever beams - Surface stress-based biosensors (SSBS)	Required fabrication of a microfluidic platform which is much complex.	Elsevier (Science Direct) Material Today Proceeding, 2018, Vol. 5, Issue 1(1), pp. 1530-1536	RM500 excluding chemical substances.

Alejandro Garcia-Miranda Ferrari, Paul Carrington (2020)	Recent advances in portable heavy metal electrochemical sensing platforms	Portable electrochemical sensors towards trace-level ion in situ heavy metal sensors	Electrode materials using Potentiostatic for Anodic stripping voltammetry and potentiometric as Ion-selective electrode.	Electrochemical methods, although suitable for in situ analysis of HM, often require expensive electrode materials and suffer from multi-elemental interferences.	Environmental Science: Water Research and Technology (RSC). 2020, J. Environ. Sci.: Water Res. Technol., 2020, Issue 6, pp. 2676-2690	Very high cost due to electrode chemical used.
Hiang Kwee Lee, Wenxiao Huang (2021)	Sensitive, portable heavy-metal-ion detection by the sulfidation method on a superhydrophobic	Portable HMI detection by sulfidation method	Sulfidation method on a superhydrophobic concentrator (SPOT) - Mobile app for on-site detection in 8 min	The development of android mobile apps to analyze chemical substances is required.	One Earth Journal by Elsevier. (2021), Vol. 4, no. 5, 1 May 2021, pp. 756–766	RM1500++ based on chemical availability.

	concentrator (SPOT)					
Subhankar Mukherjee, Soumyadeb Bhattacharyya(2021)	Sensory development for heavy metal detection: A review on translation from conventional analysis to field-portable sensor	To understand the key principles of flourishing science in HMI detection	-Electronic nose and electronic tongue sensors - Bio/chemical sensors	Optical and electrochemical-based sensors are evolving as cheaper and simpler approaches for heavy metal detection, but there is a need for increased reproducibility and anti-interference ability	Elsevier: Journal of Hazardous Materials. Trends in Food Science & Technology, vol. 109, Mar. 2021, pp. 674–689	Around RM500++

Satyam Srivastava, Vinay Sharma (2021)	Ultra-portable, smartphone-based spectrometer for heavy metal concentration measurement in drinking water samples.	Design a smartphone-based spectrometer for HMI detection.	-Handheld chemo-electronic systems with imported chemical kits -Visible spectroscopy-based sensing module with light-emitting diode and spectral sensor	The system uses off-the-shelf chemical kits for heavy metal detection, limiting its applicability to the specific metals covered by these kits.	Springer Link Applied Water Science, vol. 11, no. 11, 25 Oct. 2021	RM2000++ for each test kits and sensor cost around RM200
Tao Hu ,Qingteng Lai, Wen Fan (2023)	Advances in Portable Heavy Metal Ion Sensors	Improve the sensitivity and selectivity of sensors.	Optical and electrochemical methods, fluorescence, colorimetric, Raman scattering	Portable Raman scattering sensing often requires in situ binding of the active material to the microfluidic	Multidisciplinary Digital Publishing Institute (MDPI) Sensors, vol. 23, no. 8, 20 Apr.	Very high experiment cost if no instrument supported. (Eg: RM200k for

				channel, resulting in disposable sensors.	2023, pp. 4125–4125	fluorescence spectrophotometer)

CHAPTER 3

METHODOLOGY

In this chapter, the method on how to design a MEMs based capacitive sensors using COMSOL Multiphysics software has been carried out. Besides, the methodology also outlines the planning and procedures of project implementation. For this part also highlight the upper part of the project flow where the dimensions of the microcantilever should be first determined by analyzing the displacement of bending when force acted on it. Furthermore, the simulation of the 3D model had been carried out using COMSOL Multiphysics software and the model is created by choosing suitable material from material library hence analyze the performance and graph is plotted. Then, the process of conducting a Finite Element Analysis using different SCR in ANSYS software will be explained and the performance of the beam will then be evaluated.

3.1 Project Flowchart

The illustration of the project's workflow is shown in Figure 3.1 which includes a few steps as follows.

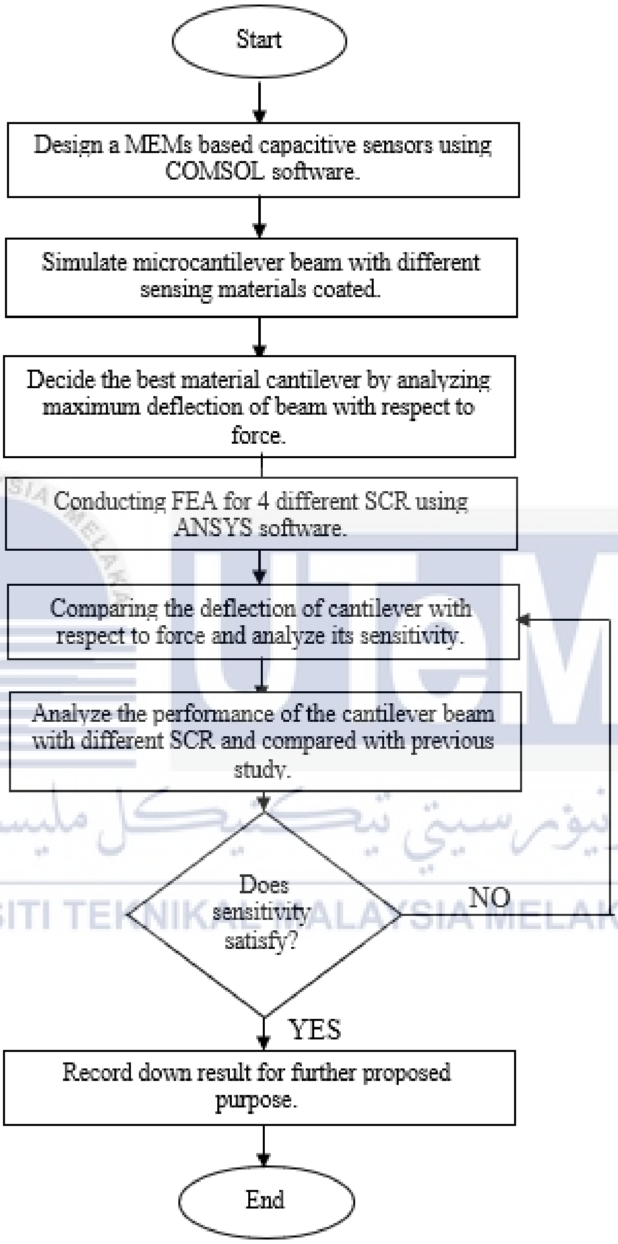

Figure 3.1: Flowchart of project handling

3.2 COMSOL Multiphysics 5.5

COMSOL Multiphysics 5.5 is a comprehensive simulation software designed to solve complex engineering problems through Multiphysics modeling. This powerful tool allows users to combine multiple physical phenomena, such as structural mechanics, fluid dynamics, electromagnetics, and heat transfer, into a single simulation environment. The software's user-friendly interface and robust solver capabilities make it an essential tool for researchers and engineers working in a variety of fields, including MEMS (Micro-Electro-Mechanical Systems), where the accurate modeling of small-scale structures like cantilever beams is crucial.

When designing a cantilever beam using COMSOL Multiphysics 5.5, users can take advantage of the software's Structural Mechanics Module. This module provides specialized tools for modeling the mechanical behavior of beams, including their deformation and stress distribution under various loading conditions. The process begins with creating a geometric model of the cantilever beam, followed by defining the material properties, such as Young's modulus and Poisson's ratio. Boundary conditions, such as fixed supports and applied loads, are then specified to simulate real-world constraints and forces acting on the beam.

The final step involves meshing the geometry to discretize the model for numerical analysis. COMSOL Multiphysics 5.5 offers advanced meshing options to ensure accuracy and computational efficiency. Once the mesh is generated, we can solve the model to obtain results such as displacement, stress, and strain distributions. These results can be visualized using COMSOL's powerful post-processing tools, allowing for a detailed analysis of the cantilever beam's performance. This comprehensive approach ensures that designers can optimize their cantilever beam designs for various applications, ranging from sensors to actuators in MEMS technology.

Figure 3.2: COMSOL Multiphysics Designing Tool

3.2.1 Design a MEMs based capacitive microcantilever using COMSOL

The design of the MEMs based capacitive sensor is based on the findings and outcomes from the related disciplined field literature reviews and research. The dimension of the microcantilever is essential to be first determined to ensure the suitability and accessibility of the project in achieving the expected outcome and design.

3.2.2 Study the effect of length and thickness of microcantilever on the performance on bending

The length and thickness of the microcantilever played an important role in ensuring the sensitivity of the beam and had enough strength to take the load of heavy metal ion. The relationship between the displacement of the cantilever with force applied on it should be determined to find the optimal dimension for the beam. Besides that, material that is used to coated on the microcantilever should be analyzed in terms of its Poisson ratio, Young Modulus, and density.

3.2.3 Design Parameters

A cantilever is a beam anchored at only one end. The beam carries the load to the support where it is resisted by moment and stress. A cantilever structure consists of greater length as compared to its width with optimal thickness. Two equations are key to understanding the behavior of MEMS cantilevers. The first is Stoney's formula, which relates cantilever end deflection 'δ' to applied stress 'σ'.

$$\delta = \frac{3\sigma(1-v)}{E}\frac{L^2}{t^2} \tag{2.4}$$

Where 'v' represents the Poisson's ratio, 'E' is Young's modulus, 'L' is the beam length and 't' is the cantilever thickness. Methods with quite sensitive optical and capacitive methods have been developed to measure changes in the static deflection of cantilever beams. The second is the formula relating the cantilever spring constant k to the cantilever dimension and material constants.

$$k = \frac{F}{\delta} = \frac{E\omega t^3}{4L^3} \tag{2.5}$$

Where F represents the force applied and 'w' is the width of cantilever. The movement of the cantilever is affected by its length, width, thickness, and various properties of the material used to make the structure. The geometric shape, as well as the material used to build the cantilever determines the cantilever's stiffness.

3.2.4 Analyze properties of different materials to give the maximum deflection of the microcantilever beam

Material properties of different materials act as a vital role in determining the maximum deflection of the microcantilever beam. Each material will have their respective properties such as Density, Young's modulus, and Poisson's ratio. All these properties will be related to Stoney's formula to find the most suitable material as the coating for the cantilever beam. Table 3.1 below shows the data for the three properties of different materials.

Table 3.1: Properties of possible coating materials.

Materials	Density (kg/m^3)	Young's modulus (Pa)	Poisson's ratio
Polysilicon	2320	169G	0.22
Silicon oxide	2200	70G	0.17
Silicon nitride	3100	250G	0.23
Gold	19300	79G	0.42
Platinum	21500	172G	0.39

According to Table 3.1 above, the properties of 3 different materials with their respective properties have been determined in COMSOL Multiphysics software to find out the most suitable materials to give maximum deflection for microcantilever. As all these properties has been combined with Stoney's formula, it is found out that the deflection of the cantilever is directly proportional to the density of the material chosen and inversely proportional to the Young's modulus so to achieve a maximum deflection, large density of material with low Young's Modulus should be chosen. Hence from calculation the most suitable material is silicon oxide, and it is found to be the best analysis film for further simulation.

▼ Material Contents

	Property	Variable	Value	Unit	Property group
☑	Density	rho	2200[kg/m^3]	kg/m³	Basic
☑	Young's modulus	E	70e9[Pa]	Pa	Young's modulus and Poisson's ratio
☑	Poisson's ratio	nu	0.17	1	Young's modulus and Poisson's ratio
	Electrical conductivity	sigma_iso ; s...	0[S/m]	S/m	Basic
	Coefficient of thermal expansion	alpha_iso ; a...	0.5e-6[1/K]	1/K	Basic
	Heat capacity at constant pressure	Cp	730[J/(kg*K)]	J/(kg·K)	Basic
	Relative permittivity	epsilonr_iso...	4.2	1	Basic
	Thermal conductivity	k_iso ; kii = k...	1.4[W/(m*K)]	W/(m·K)	Basic

Figure 3.3: Properties of Silicon oxide in COMSOL software.

3.2.5 Building a microcantilever beam with load and mesh process

As the parameter of the designed microcantilever beam that shown in Table 3.2 has been built accordingly, then several steps need to be taken before conducting the simulation and performance analysis.

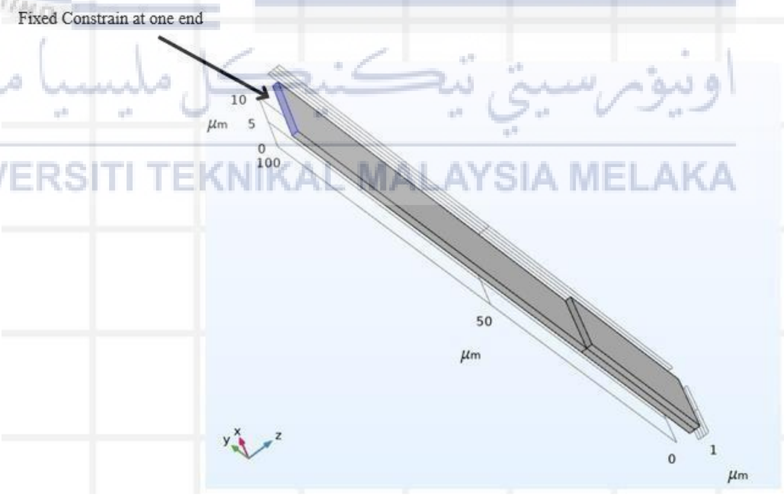

Figure 3.4: Fixed Constrain at one end of the cantilever beam.

Figure 3.4 above shows the first action that needs to be taken which is making one side end of the beam to be fixed constrain. The purpose of doing this is to ensure that the cantilever beam can deflect when the load is applied to another end of the beam.

Next, a load will be applied to another end of the beam or so called the sensing area of the beam.

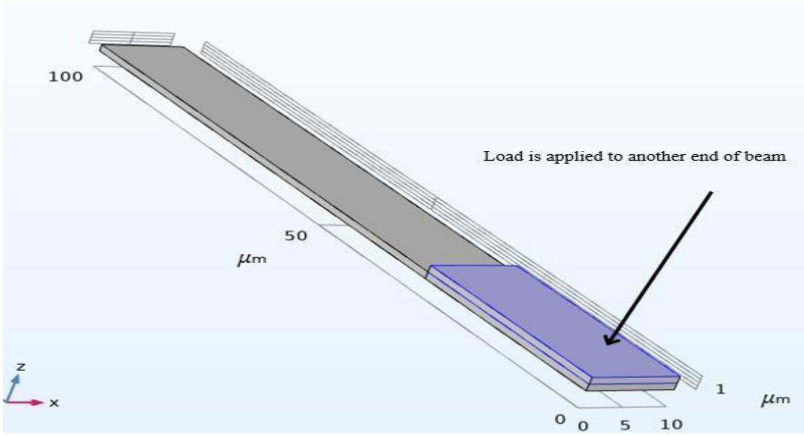

Figure 3.5: Load applied to another end of the beam

Figure 3.5 above shows that the load is being applied to the end of the beam to act as the force that acts on the cantilever beam and cause the beam to deflect. A range of 0.1μN-3μN of force will be simulate on the beam and the performance of the beam will be analyze based on different materials used to coat on it and the deflection of the beam will be observed and recorded.

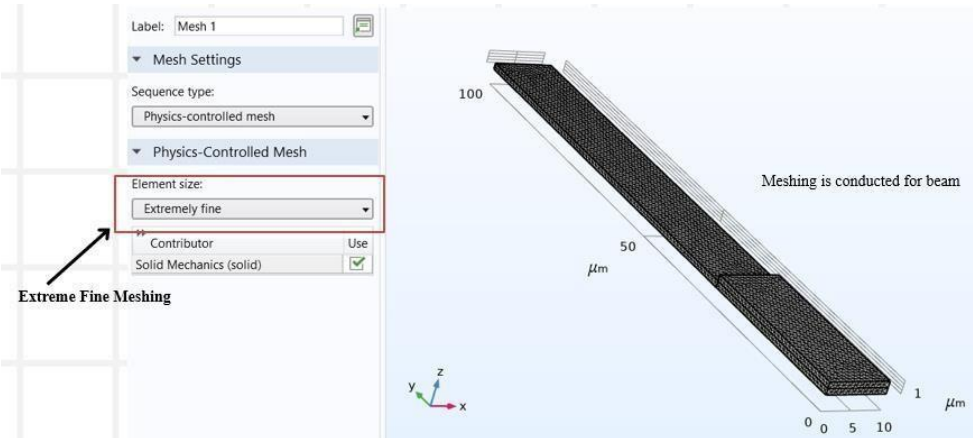

Figure 3.6: Meshing process with element size defined.

After the process of fixed constrain and load applied has been done, the process of meshing will be then conducted. This process is essential for defining the element size as it will convert the geometric model into a finite element model that can be used for numerical analysis. The sequence type that had been implemented in this design is Physics-Controlled Meshing where this is a straightforward option where COMSOL automatically determines the appropriate mesh based on the physics involved and the geometry of the model.

The element size will be crucial in the mesh as it significantly affects the accuracy and efficiency of the finite element analysis. Extremely fine size had been chosen in designing the cantilever beam because using smaller elements generally increases the accuracy of the simulation because they can more precisely capture the gradients and variations in the physical fields such as stress and temperature across the geometry. This is especially important in regions with high stress concentrations or complex boundary conditions.

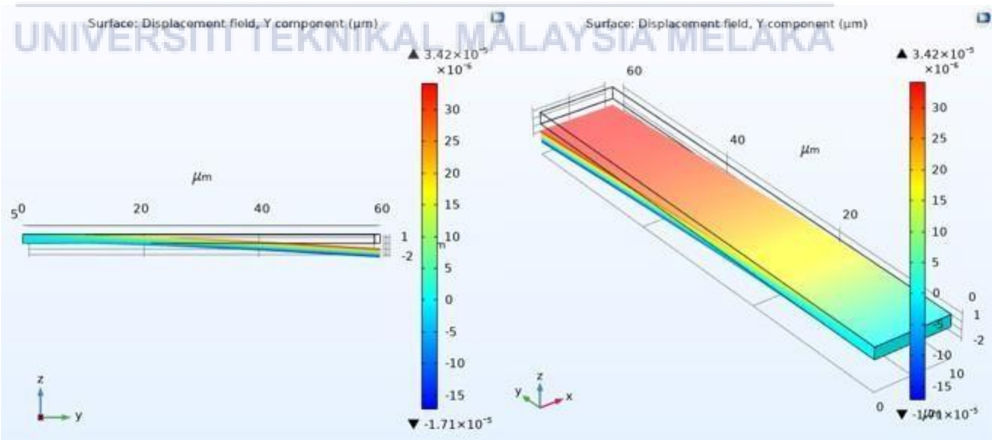

Figure 3.7: Deflection plot with 500Pa load acted on the boundary.

Figure 3.7 above shows the example of the simulation result when the cantilever beam is undergoing statistical test after the pre-processing designing steps have been done. As it can see the beam will deflect only one side because the other end has been fixed and the result showing includes the force distribution that acts on the beam and which part of the beam will result the highest stress and lead to higher deflection.

Table 3.2: Parameter of the designed microcantilever beam.

Parameter	Expression	Value (μm)
Width	10e-6	10
Length	100e-6	100
Thickness	1e-6	1

3.3 Optimization of Capacitive microcantilever beam

The previous study stated that the dimensions of the microcantilever beam played an important role in determining the sensitivity of the beam and the need to ensure that it will not break when a load is applied on it in future time. Hence, a fixed beam is created to simulate different kinds of dimensions which are related to the deflection which respects the force. First, a block needs to be created as the geometry shape to simulate as the real microcantilever beam then a material should be chosen from the library as the results obtained in earlier stage for the best material to suit the design that will bring maximum deflection without breaking. Then a fixed constraint should be applied to one end of the block to ensure that experiment on deflection would occur on the other end of the block with one side fix. Then the boundary load was chosen to act on the surface of the cantilever with value defined. After that, the level of mesh is defined to approximate the CAD geometry and it represents the discretization part of computing finite element methods as the higher the resolution of discretization, the finer the error in simulation. Then the geometry can be now computed and observe the output which is the displacement graph of the cantilever. The maximum deflection will depend on the value of displacement versus force. Then the steps will be repeated by varying the length and thickness to find the best dimension of the microcantilever beam.

3.4 Ansys Workbench 2024 R1

ANSYS software is a powerful tool for performing detailed simulations and analyses of engineering structures, including cantilever beams. When designing a cantilever beam with different SCR (Stress Concentration Region) holes in ANSYS, the software provides a comprehensive environment to model, analyze, and optimize the beam's performance under various loading conditions.

The process of developing a microcantilever beam using Ansys Workbench will be quite like COMSOL Multiphysics but in terms of the steps on creating the beam sensor will be slightly different by implementing in both software. This includes defining the dimensions of the beam and the different types of SCR holes, such as circular, triangular, or octagonal. Once the geometry is created, material properties like Young's modulus and Poisson's ratio are specified. Boundary conditions are then applied to fix one end of the cantilever, ensuring it remains immobile under applied loads. These boundary conditions are critical as they mimic real-world constraints, ensuring that the simulated results accurately reflect the beam's behavior in actual applications.

Next, still the process of meshing will be done but unlike COMSOL software that the ultra-fine mesh properties can be defined on the beam to ensure the force distribution will be very even when the simulation was undergo after force applied but for ANSYS software there are only a default mesh can be implemented hence the sensitivity of the beam including the result of deflection will be different for both software even though the dimension and material used to coated on the beam was the same but this factor will still affect the result observed.

Figure 3.8: ANSYS Workbench Simulation Tool

3.4.1 Finite Element Analysis with different SCR in ANSYS software

The analysis is carried out to investigate and understand the stress and deflection of the MEMs based microcantilever sensor when load is applied on it and in this case, assume that the load represents different types of Heavy Metal Ions with respective properties. The model block will be first imported from COMSOL Multiphysics software into ANSYS software to ensure that there will be no error during analysis. The SCR's parameters will be examined to improve deflection sensitivity. Static analysis and modal analysis were the two forms of analysis that were done. To model the stress created when a load is placed precisely at the edge of the beam with the other end fixed, static analysis was carried out using element type SOLID5. On cantilever beams with a rectangular shape, this was done. Two distinct static analyses, denoted by the vertical displacement and vertical force, were conducted. The average stress was calculated using the stress values that ANSYS had simulated. This stress value was then utilised to determine the piezoresistive displacement and force sensitivity.

3.4.2 Element Type

Selecting the appropriate elements is crucial to ensure the desired analysis is achieved. The chosen element must be elastic, exhibit consistent performance, and be compatible with computer capabilities. Various types of elements have been tested to suit the MEMS cantilever models, with results verified alongside computer performance to ensure precise analysis.

3.4.3 Material properties

For this analysis, linear material properties are used in both models. Linear properties are chosen because they require only a single iteration for analysis and are not temperature dependent. Additionally, the material is defined as isotropic, meaning it exhibits the same mechanical properties in all directions. Silicon oxide will be used during the analysis of the microcantilever as the coating material on heavy metal ion detection. Table 3.3 below shows the material properties of silicon oxide.

Table 3.3: Material properties of silicon oxide

Properties	Value
Young’s Modulus	70GPa
Poisson Ratio	0.17
Density	2200 kg/m^3

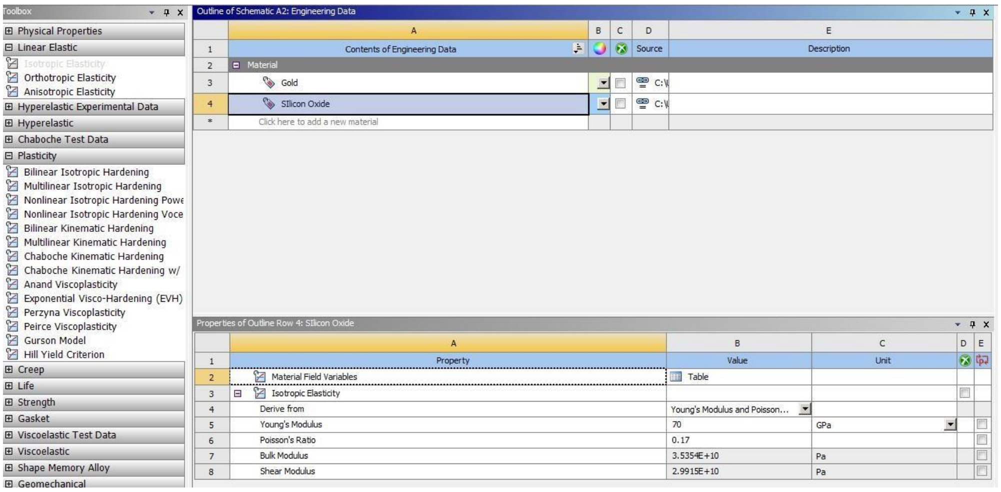

Figure 3.9: Material properties defined and selected

Figure 3.9 above shows the material properties in the engineering data window where there are tons of materials that can be selected from the database but also a manual defined mode on defining specific materials. In this case, few materials will be used in analyzing the performance of the cantilever beam including silicon oxide, silicon nitride, gold, polysilicon, and platinum. All the materials will be defined in terms of Young's Modulus and Poisson's ratio. After all the materials parameters have been defined it will then be stored inside an engineering database for future use.

3.4.4 Model creation

The next step is to model creation part inside the model window. In this part, the dimensions used will be the same as the model designed using COMSOL software including the sensing area.

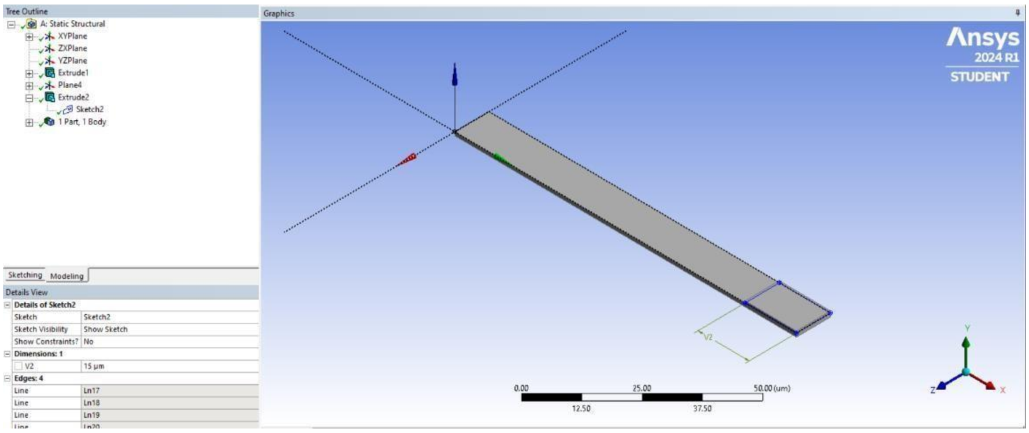

Figure 3.10: Model created in ANSYS

3.4.5 Meshing

Accurate meshing is essential for reducing the time and effort required to obtain precise results. In computational analysis of structural or fluid simulations using Computational Fluid Dynamics (CFD) or Finite Element Analysis (FEA), meshing plays a critical role. The mesh breaks down the object to be simulated into smaller cells, which accurately define the geometry of the object. This detailed representation ensures that the computational analysis can produce reliable and accurate results. Different levels of mesh such as fine mesh, or superfine mesh should be first declared for the designing of a microcantilever beam to provide an accurate result on deflection with respect to force applied on it.

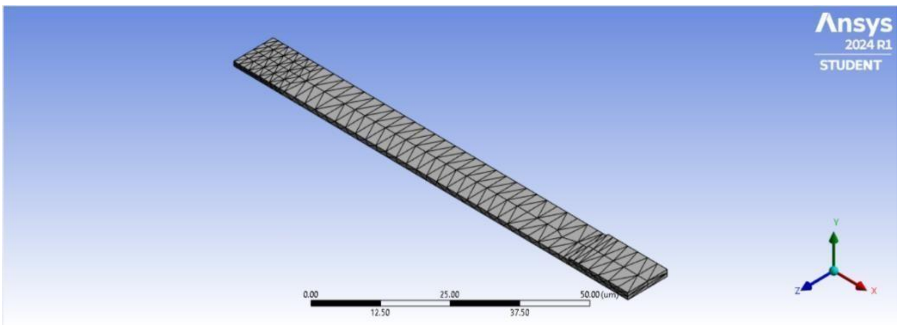

Figure 3.11: Element plot after meshing for cantilever beam

3.4.6 Boundary Conditions

Boundaries or restrictions must be put in place before solutions may be implemented. Boundary conditions specify regions or bodies that are fixed and cannot move in any direction or degree of freedom (DOF). The areas with boundary conditions ensure that there is no deflection or movement when a load is applied.

Boundary conditions or limitations are commonly referred to as loads in ANSYS software. This involves applying additional loads, both internal and external, as well as boundary conditions including supports, limitations, and boundary field specifications. These loads can be applied to nodes and elements in the finite element models, or to critical points, lines, regions, and volumes in the solid model.

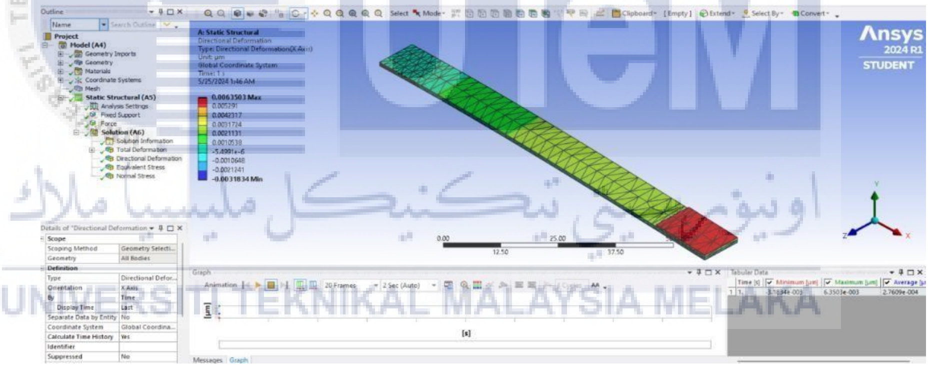

Figure 3.12: Deflection Analysis after boundary conditions set

As Figure 3.12 above showing the analysis and setup in geometry site where first we will import the geometry that has been created then the material will be selected to coated on the beam and undergo different simulations. Next, meshing process will also be defined as in COMSOL software but different in terms of the element size.

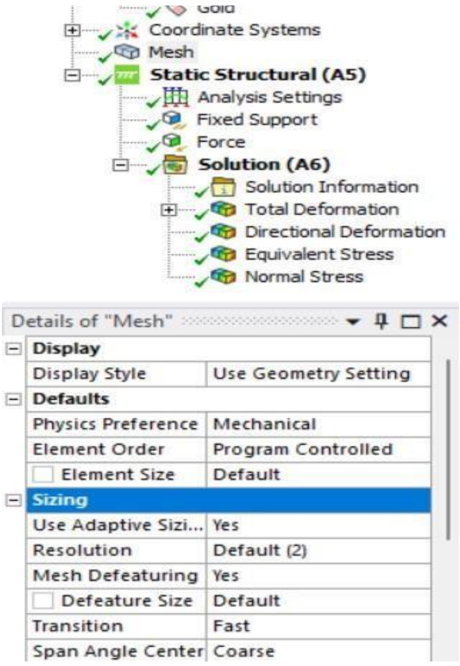

Figure 3.13: Default mesh for cantilever beam in ANSYS

After the mesh has been defined and generated as shown in Figure 3.11, it will then move to the static structural on the analysis setting which include the fixed support and force applied to 2 ends of the cantilever beam. The assumption parameter will remain the same for force applied which will be vary from 0.1µN - 3µN. Few parameters including total deformation, directional deformation, equivalent stress, and normal stress will be analysed and evaluated using all the materials.

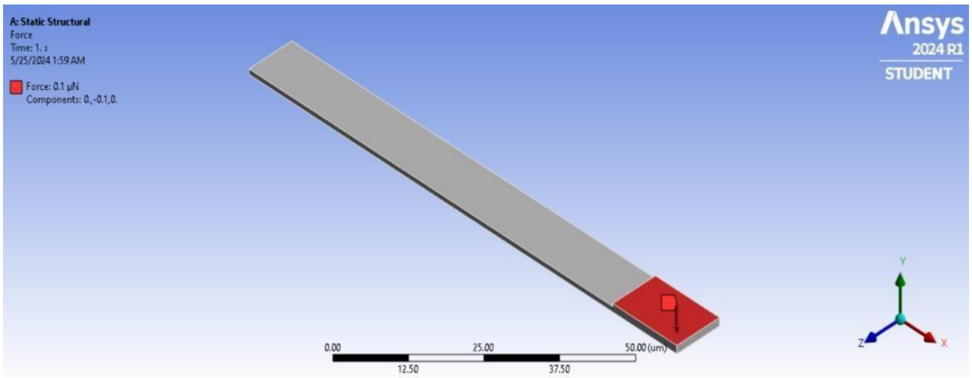

Figure 3.14: Force applied on the sensing beam

3.5 Stress Concentration Region on cantilever performance

Different types of SCR will be implemented to determine the best shape placed on the cantilever that will result in the best performance. This includes a circular stress concentration region where it introduces a circular hole or notch at a specific point along the beam and it may induce stress concentrations at the edges, causing higher stress levels compared to the surrounding material.

Next, hexagonal SCR will create a hexagonal cutout or protrusion in the beam and since a hexagonal shape with sharp edges, can lead to the stress will mainly be focused on these edges and affect the stress distribution hence led to the change in deflection of the beam. The analysis will be conducted using square, triangular, and rectangular SCR with implement a respective shapes or cutout on the beam and induce different stress concentrations according to the shapes design.

The stress distribution when a load act on the beam especially when a heavy metal ion placed on it will also affect the result observed based on the deflection of the beam with respect to the stress concentration region applied hence it is essential to analyze the best shape of the region to indicates the best sensitivity for the microcantilever beam on HMIs detection.

Table 3.4 summarizes the analysis results of surface stress or average stress difference for various types of SCR holes. The results indicate that as the number of sides of the SCR holes increases, the surface stress also increases. The octagonal SCR holes generate the highest stress because they have the most sides, which contributes to increased surface stress. He and Li (2006) further investigated the effect of adding more octagonal holes to the cantilever. Table 4 displays the surface stress at SCR holes when different numbers of SCR holes of the same size are added along the length of the cantilever, with equal spacing between the holes. The data show that adding more SCR holes does not enhance surface stress. Therefore, a single octagonal SCR hole is sufficient to maximize surface stress.

Table 3.4: Maximum stress for different shape of SCR holes

Shape of SCR holes	Maximum Stress (MPa)
Cantilever without any hole	439
Rectangular	589
Square	563
Hexagonal	591
Octagonal	690
Circular	621
Elliptical	590

Besides that, there are also a few types of SCR simulation that has been done by Joshi et al. (2007) and showing the result of the maximum stress observed by implementing different types of SCR to the cantilever beam. Figure 3.15 below shows the result of the maximum stress observed.

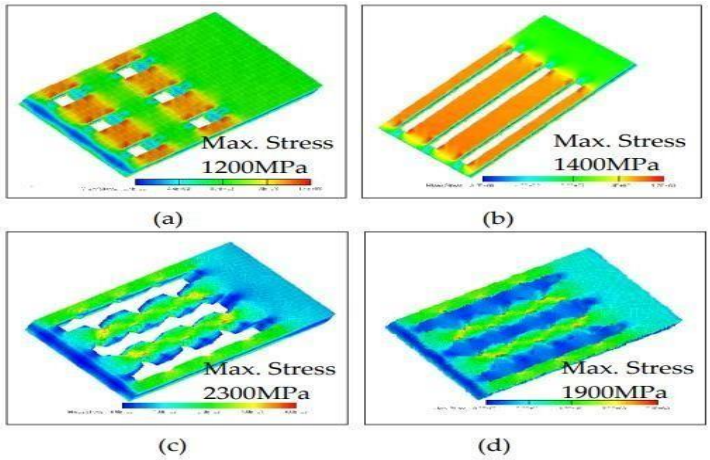

Figure 3.15: Analysis of different SCR resulting in different maximum stress

3.6 Summary

The design of the capacitive microcantilever beam is discussed and clarified in this chapter and the way on designing and deciding the suitable dimension using COMSOL Multiphysics software. The analysis process is repeatedly carried out until the best dimension of the microcantilever beam has been decided and can be used for further Finite Element Analysis with different types of HMIs and their respective mass using ANSYS software. It is vital to create a sensitive sensor and optimize the existing cantilever to achieve better results with the best dimensions and material chosen.

CHAPTER 4

RESULTS AND DISCUSSION

This chapter presents the results and findings obtained in the implementation of this project. It clearly sets up the expected and experimental results and analyses the related performance of the microcantilever beam that designed using 2 different structural analysis software which are COMSOL Multiphysics and ANSYS Workbench. This 2 software will be effective in conducting structural analysis of the beam along with finite element analysis that can clearly show the performance of beam according to different parameter setting and material properties. This will be much helpful in future fabrication process for heavy metal ion detection using microcantilever beams sensor. It also discusses the environmental and sustainability features of this project. The objective of this study was to confirm the findings in Chapter 3 to demonstrate the program's comparability and dependability.

4.1 Microcantilever beam built in COMSOL Multiphysics

The purpose of conducting a simulation using COMSOL software is to analyze the dimensions of the microcantilever beam along with the material that is most suitable for material sensing in terms of its deflection. Therefore, it is essential to define different types of materials that are possible to result in maximum deflection that related to Stoney's formula.

First a rectangular beam was built according to the parameters set in Table 3.2 and to ensure the sensitivity of the microcantilever beam, the thickness of the beam was set to 1µm to result in maximum deflection when force applied.

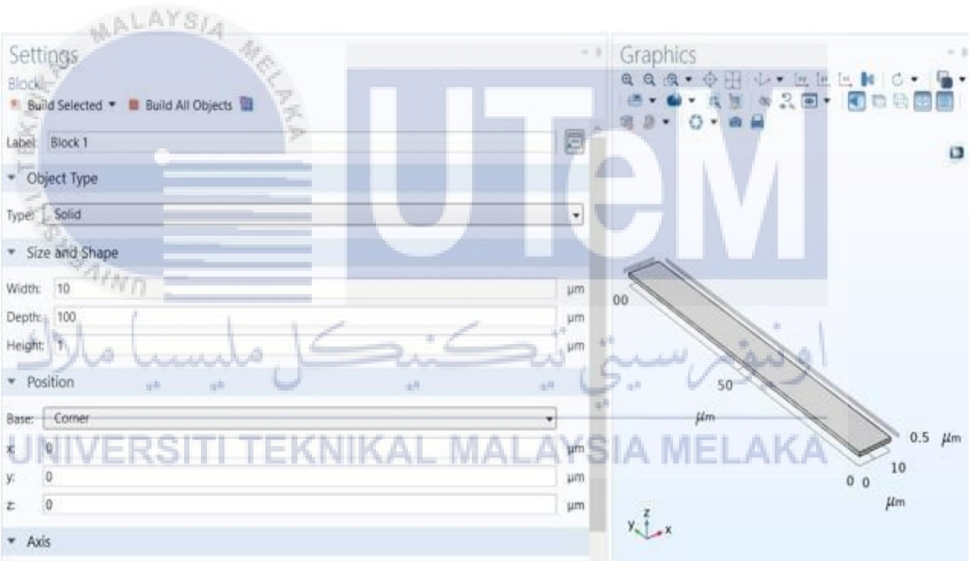

Figure 4.1: Rectangular cantilever beam built in COMSOL Multiphysics software

The beam has then been modified by adding a sensing beam at the end of the beam with a length of 30µm and a thickness of 1µm.Figure below shows the beam that has been rebuilt after defining a second block and added on the top of the first beam to act as the sensing area for simulation later. The height showing in represents the total thickness of both beam which are 1µm thick each to ensure the sensitivity and deflection can reach its maximum limit.

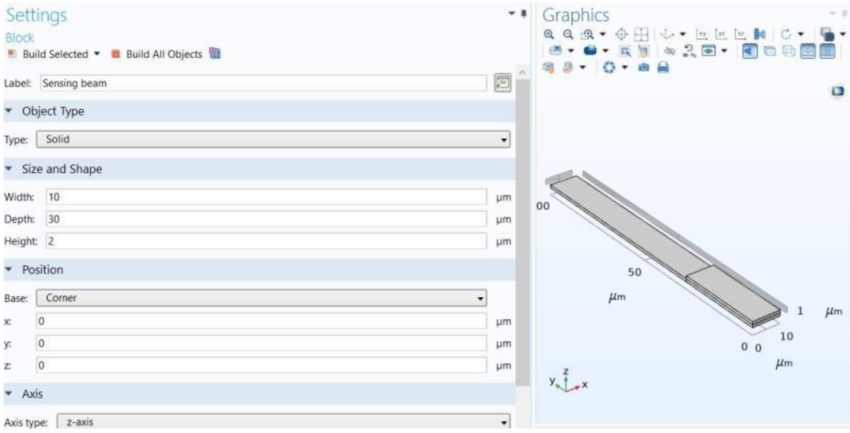

Figure 4.2: Sensing beam built in COMSOL

4.2 Boundary Conditions on two ends of beam

Boundary conditions are set based on two parameters which are fixed constraints and Boundary load. For fixed constraints that are shown in figure below, there are few purposes for implementing this action. This includes simulating the real-world constraints. Fixed constraints represent points or surfaces in a structure that are immobile. This is crucial for accurately modeling how a structure interacts with its supports or foundation. For instance, in a cantilever beam, the fixed end simulates the support that holds the beam in place and prevents any movement.

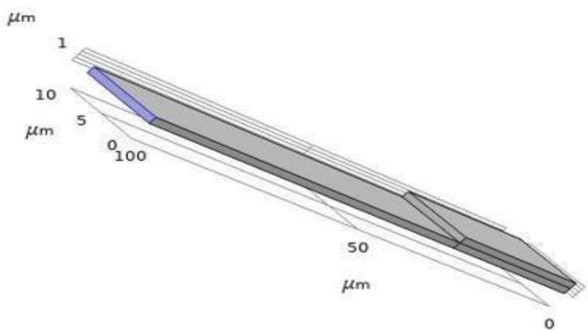

Figure 4.3: Fixed constraints boundary conditions

Moreover, it can also prevent rigid body motion. Without fixed constraints, a structure in a simulation might experience rigid body motion, which means it could move freely in space without any deformation, leading to unrealistic results. Fixed constraints ensure that the structure remains in place and that any applied loads result in deformation rather than translational or rotational movement of the entire structure.

Therefore, it is extremely crucial in finite element and structural analysis to enable accurate load applications, providing reliable and meaningful simulation results. Next, a boundary load was applied to the sensing beam as shown in Figure 4.4 below.

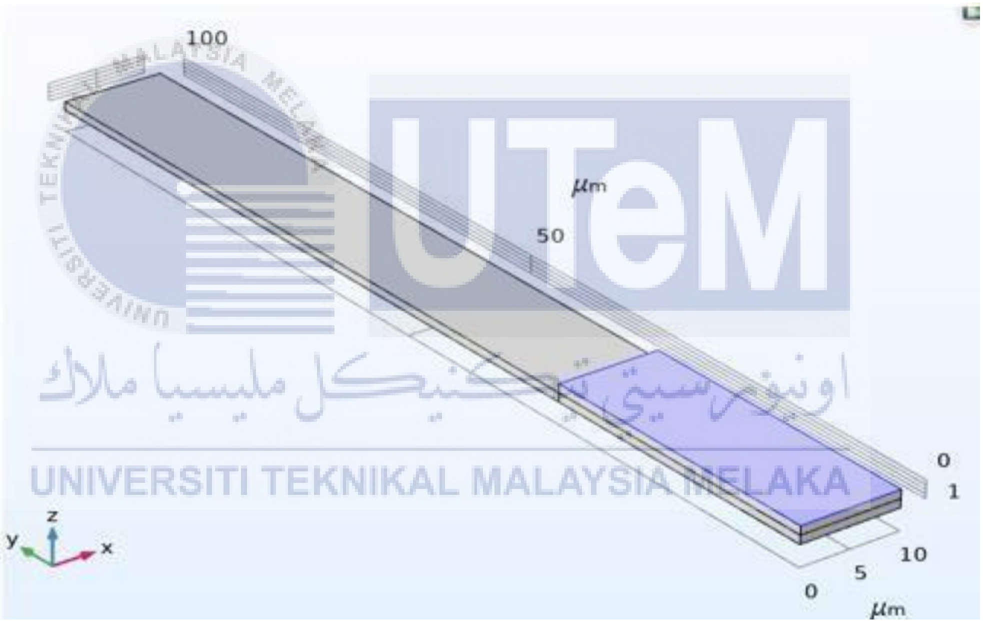

Figure 4.4:Boundary load condition onto the sensing beam

From above, the load is applied to the sensing area of the microcantilever beam, and the force applied on it will vary from 0.1µN-3µN. This will ease understanding and analyzed on the performance with various conditions especially dealing with heavy metal ion in future time.

4.3 Different materials properties and its expected results

Material played an important role in designing a microcantilever beam especially when it comes to the performance analysis. Each material will have their respective elastic properties so it may affect the curvature and deflection of the beam. Table 4.1 below shows the elastic properties of various materials that has been selected and compared in deflection simulation.

Table 4.1: Elastic properties of different materials

Materials	Young's modulus (Pa)	Poisson's ratio
Polysilicon	169G	0.22
Silicon oxide	70G	0.17
Silicon nitride	250G	0.23
Gold	79G	0.42
Platinum	172G	0.39

To result in maximum deflection, Stoney's formula was taken into account and consideration and according to the formula, a lower Young Modulus and Poisson Ratio will result in the maximum deflection theoretically, therefore it is expected thatthe material of silicon oxide will perform the best and giving a higher deflection compared to other materials since it has the lowest value of Young Modulus at 70GPaand 0.17 Poisson ratio.

Table 4.2: Maximum deflection with force applied for different materials.

Force (µN)	**Maximum Displacement (µm)**				
	Silicon Nitride	**Silicon Oxide**	Polysilicon	Gold	Platinum
0.1	0.06	**0.21**	0.09	0.19	0.09
0.5	0.3	**1.07**	0.44	0.96	0.47
1	0.6	**2.13**	0.88	1.92	0.93
1.5	0.89	**3.2**	1.32	2.88	1.4
2	1.19	**4.27**	1.76	3.84	1.86
2.5	1.49	**5.34**	2.2	4.8	2.33
3	1.79	**6.4**	2.64	5.76	2.8

The table above shows the results obtained from COMSOL Multiphysics software with the simulation on the designed microcantilever beam by using different coating materials. The maximum deflection of the beam was analyzed by varying the force applied to one end of the beam to simulate the real weight of the heavy metal ions acting on it. The results were obtained based on the maximum displacement of the beam, and it is proportional to the properties of the materials. The best material should be found before further analysis is conducted to give the best sensitivity and accuracy of the sensor beam.

Figure 4.5 below shows the tabulated graph for different materials on their deflection which coated on the beam.

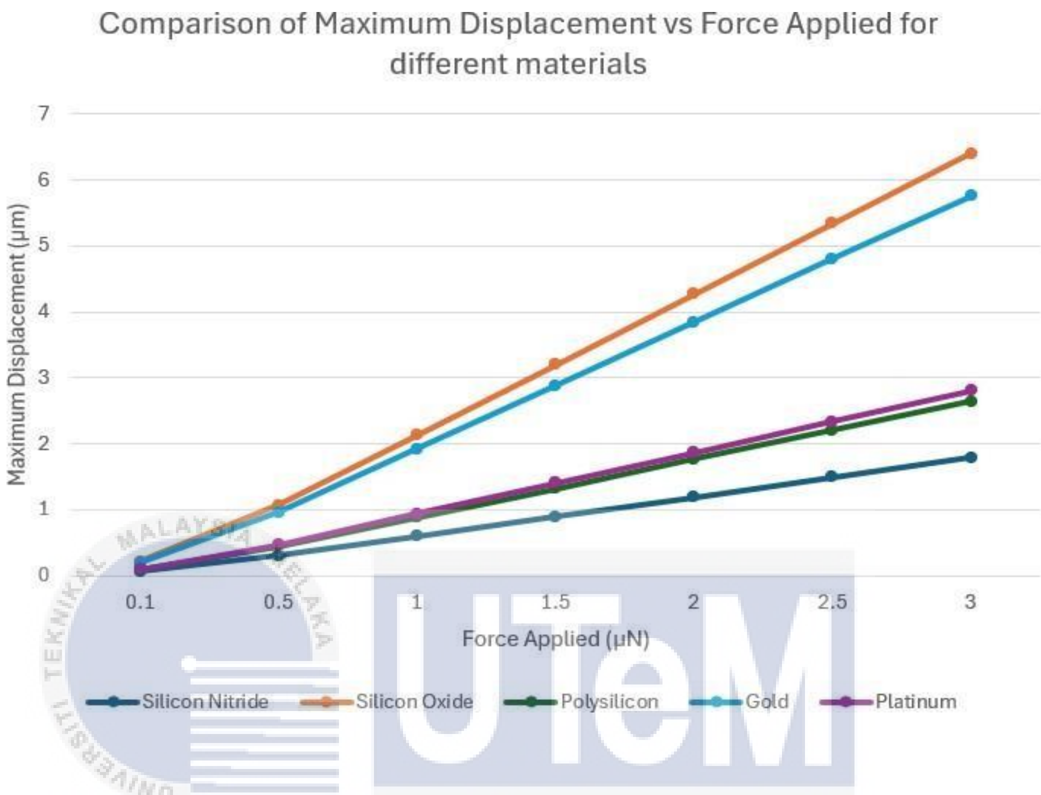

Figure 4.5: Line graph of force applied vs Maximum deflection of the beam for different materials.

Based on the line graph above that shows the deflection of silicon oxide cantilever beam result the highest value followed by gold, platinum, polysilicon and silicon nitride and this result fulfill the expected outcome which mentioned in earlier this section. Therefore, this can conclude that the material Silicon Oxide represents the most suitable material for conducting Finite Element Analysis.

4.4 Comparison on the performance of microcantilever beam

The designed microcantilever beam will be further analyzed by implementing different Stress Concentration Region (SCR) using ANSYS Workbench software but to ensure that the designed cantilever beam will have better performance compared to previous study with new dimensions and sensing beam added. The deflection comparison was shown in Table 4.3 below.

Table 4.3: Performance comparison on the beam deflection

Material	Previous study (µm) S. Syed (2016)	**Current study (µm)**	Percentage improvement (%)
Silicon Oxide	27.577	**28**	1.51
Polysilicon	11.984	**12.1**	0.96
Gold	25.739	**26.0**	0.01

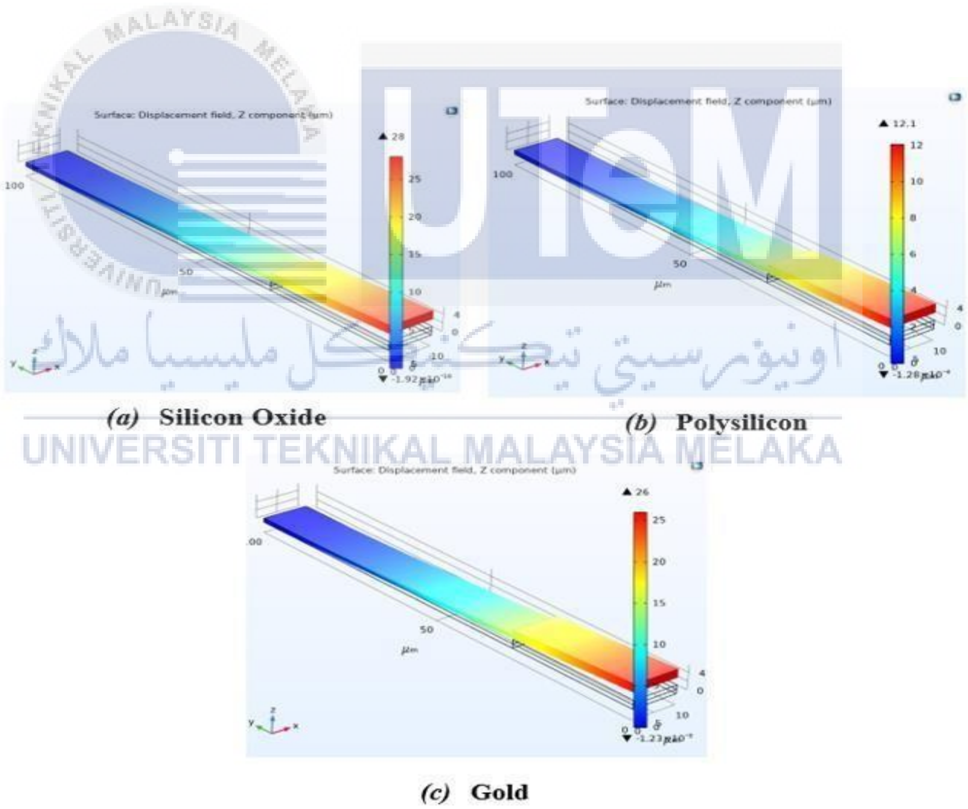

Figure 4.6: Result of deflection with 3 different materials

From Table 4.3 the result obtained by S.Syed (2016) using three different materials as same as the current study in this paper but differ in terms of the dimensions of the beam and types of meshes that had been generated [32]. According to Table 4.3, the results obtained were all based on a force of 5µN that act on the sensing beam. From Figure 4.6 it shows the simulation result of three materials with their respective deflection when the force is applied on it. It is obviously showing the result that Silicon Oxide will still provide the maximum deflection followed by gold and polysilicon. These results fulfilled the conditions and parameters that had been assumed in section 4.3.

The simulation result was improved by approximately 1.5% for silicon oxide, 0.96% for polysilicon and 0.01% for gold materials. The results were not much different but still there is minor improvement for current design since the dimensions of the beam were different also the meshing size of the beam will be unlikely too. All these factors will bring effect to the number of deflections of the beam therefore it is crucial to analyze the suitable dimensions and design to achieve the highest sensitivity of the beam.

As for now, the most suitable dimensions of the beam along with materials has been achieved and found out to result in higher deflection compared to previous study. Next, the designed beam will be again analyzed using ANSYS Workbench software in terms of FEA using different types of SCR. The performance of the beam will then been evaluated and compared with previous study too to investigate whether this design will perform better with Stress Concentration Region included.

4.5 FEA in ANSYS Workbench

Using static structural analysis in ANSYS Mechanical, which employs the ANSYS solver, performed structural analyses to determine the Equivalent Elastic Strain, Equivalent Stress, and total deformation in structures or components subjected to loads. These loads did not induce significant inertial and damping effects, as assumed in a static analysis context. For this analysis, a few types of SCR were used to analyze the performance of the microcantilever beam such as Rectangular, Circular, Triangular, and Square.

This static structural analysis was to evaluate the Equivalent Elastic Strain, Equivalent Stress, and total deformation under the applied load. Equivalent elastic strain measures the material's reversible deformation, while equivalent stress, often calculated using the von Mises stress criterion, indicates the stress state within the material. Total deformation refers to the overall displacement experienced by the structure. The presence of SCR may affect the localized deflection and influence the overall deflection since the presence of high-stress region may cause the redistribution of load and leading to a non-uniform deflection profile along the length of the beam.

To perform a Finite Element Analysis with different Stress Concentration Region to the microcantilever beam that had been designed using COMSOL Multiphysics software with suitable dimensions and materials selected, there are still several steps that need to be follow as shown below:

1. Defining Engineering Data for various material in terms of its elastic properties such as Young Modulus and Poisson Ratio.
2. Sketch the model according to dimensions setting in Table 3.2 along with the sensing beam.

3. Geometry built up with various boundary conditions declared including meshing, analysis setting such as fixed support and force applied.
4. Create different kinds of hole such as rectangular, circular, triangular, and square on the surface of the cantilever beam to act as the stress concentration region.
5. Analyzed the performance of the cantilever beam by varying the force from 0.1µN-3µN.
6. Observed the solutions in terms of Total Deformation, Directional Deformation, Equivalent Stress, and Normal Stress.

4.6 Stress Concentration Region Built

The microcantilever beam was first built according to dimension and materials defined. After that, a stress concentration region was built on the surface of the beam.

Figure 4.7 below shows the microcantilever beam in ANSYS software with and without a rectangular hole or known as the stress concentration region.

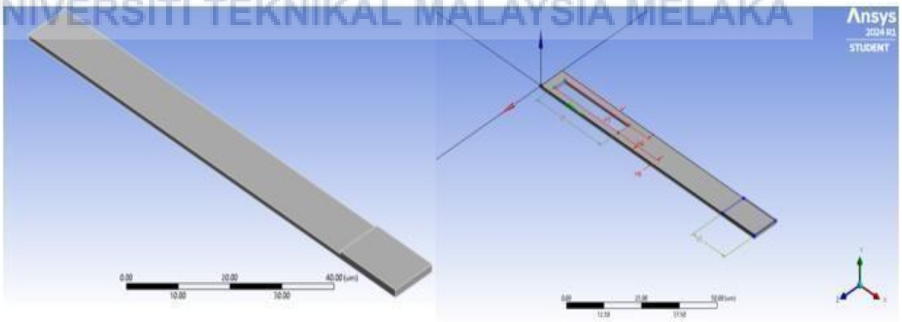

Figure 4.7: Microcantilever beam with and without SCR

Figure 4.7 represents the designed cantilever beam with and without Rectangular Stress Concentration Region and the deflection of the beam are differ from previous result since the load and stress distribution along the beam has been change therefore the performance will be observed and evaluated started from section 4.6.1 with various SCR changes including rectangular, circular, triangular, and square respectively. Since the material has been selected and justified using COMSOL Multiphysics software, in this section all the beams are evaluated using Silicon Oxide material, but overall result data are tabulated for all materials including both with and without Stress Concentration Region.

4.6.1 Performance of cantilever with Rectangular SCR

The performance of the microcantilever beam was simulated using ANSYS software with a rectangular SCR. The dimensions of this rectangular hole will be 30x5x1μm. Figure 4.8 below shows the geometry imports to the model space for further analysis along with rectangular SCR hole.

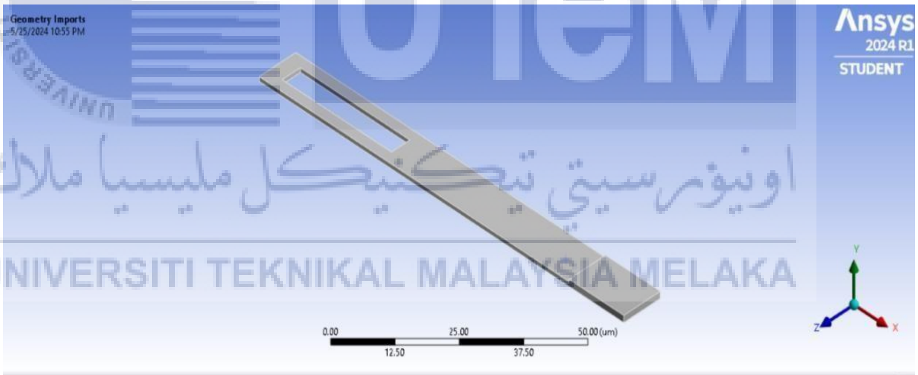

Figure 4.8: Geometry imports with rectangular SCR

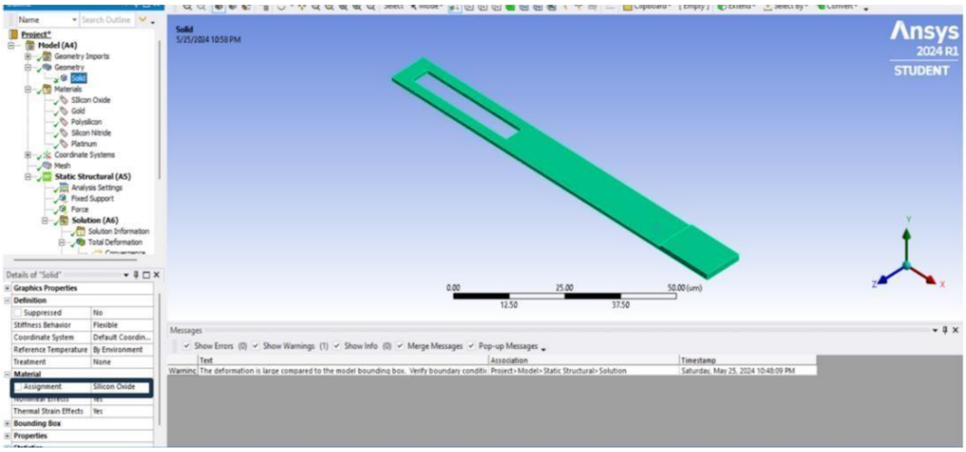

Figure 4.9: Material Assignment of Silicon Oxide

After the geometry has been import with material assigned, the beam will then be simulated through a range of force from 0.1 µN - 3 µN. A few parameters will be observed and evaluated based on this Stress Concentration Region and make a comparison for the result of maximum deflection between the existing of SCR and without SCR to see whether this SCR hole help to improve the sensitivity of the beam.

Table 4.4: Maximum result of cantilever beam with Rectangular SCR

Force (µN)	Silicon Oxide		
	Maximum Deflection (µm)	Equivalent Stress (MPa)	Shear Stress (MPa)
0.1	0.8407	12.6562	0.6766
0.5	4.2037	63.281	3.3828
1	8.4073	126.56	6.7657
1.5	12.611	189.84	10.148
2	16.8148	253.124	13.531
2.5	21.0185	316.405	16.914
3	25.2222	379.686	20.2968

Table 4.4 above shows the simulation results for silicon oxide coated beam with a rectangular Stress Concentration Region. For 0.1 µN of force applied, the microcantilever beams record a maximum deflection of 0.8407 µm and as the force keep increasing, the amount of deflection will be increase as well to a value of 25.2222 µm when 3 µN load has applied on it. Figure 4.10 below shows the deflection plot along with the stress distribution along the beam. The red colour region represents the maximum stress that acts on the beam which is the sensing area. The stress concentration region helps in distributing the load evenly compared to a normal beam.

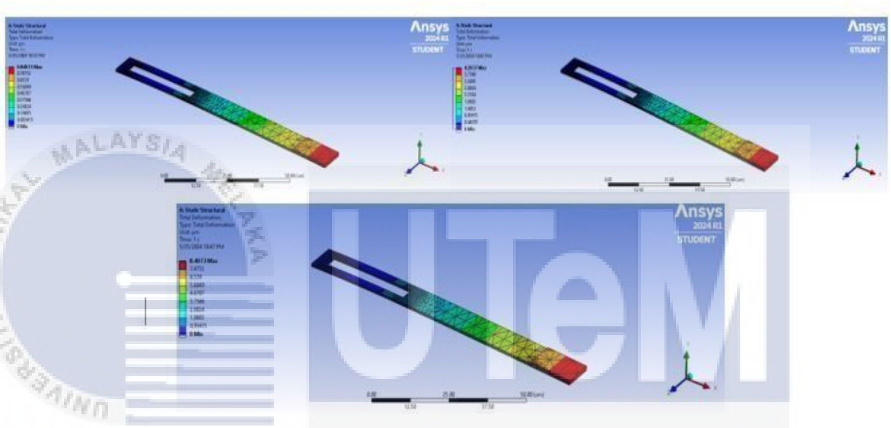

Figure 4.10: Maximum Deflection for Rectangular SCR

To analyze the performance of the beam without SCR, the result using same parameter, but the difference is by using a plain cantilever beam without SCR and the results was simulated then recorded in Table 4.5 below.

Table 4.5: Maximum results without Rectangular SCR

Force (μN)	Silicon Oxide		
	Maximum Deflection (μm)	Equivalent Stress (MPa)	Shear Stress (MPa)
0.1	0.5049	5.436	0.72366
0.5	2.5249	27.18	3.683
1	5.0498	54.36	7.2366
1.5	7.5747	81.54	14.6026
2	10.0996	108.72	18.2856
2.5	12.6245	135.9	21.9686
3	15.1494	163.08	25.6516

Table 4.5 above shows that the maximum deflection without Rectangular SCR has been reduced compared to the SCR present cantilever beam. Therefore, it can be concluded that the presence of Stress Concentration Region will increase the sensitivity of the cantilever beam.

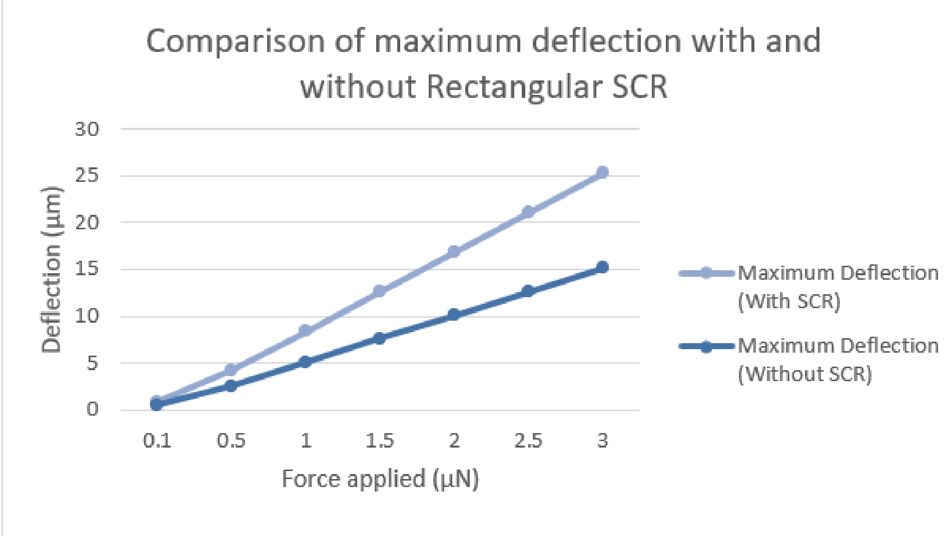

Figure 4.11: Graph of comparing performance of beam with and without Rectangular SCR

Figure above represents the graph plot showing the results obtained from simulation according to the presence of SCR. It can be noted that the deflection of the beam will be higher with SCR compared to the plain microcantilever beam.

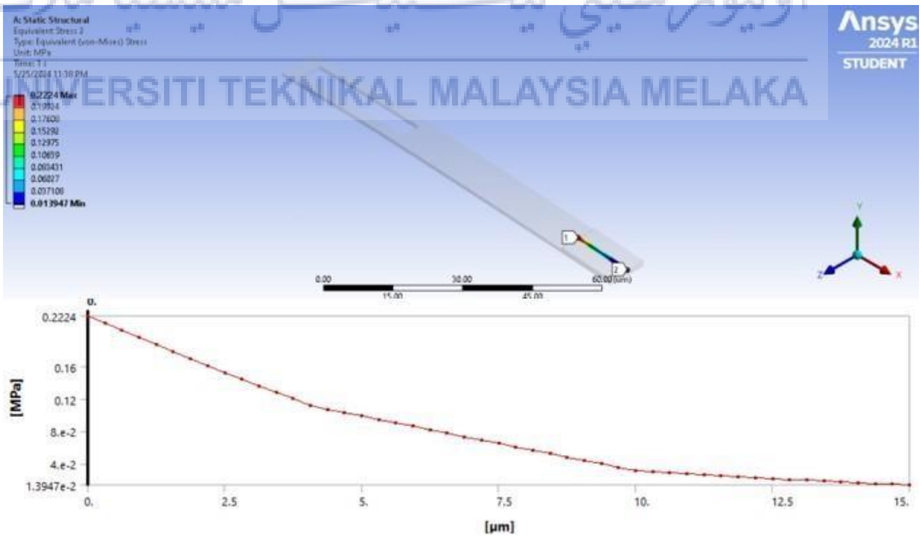

Figure 4.12: Directional Deformation along the sensing beam

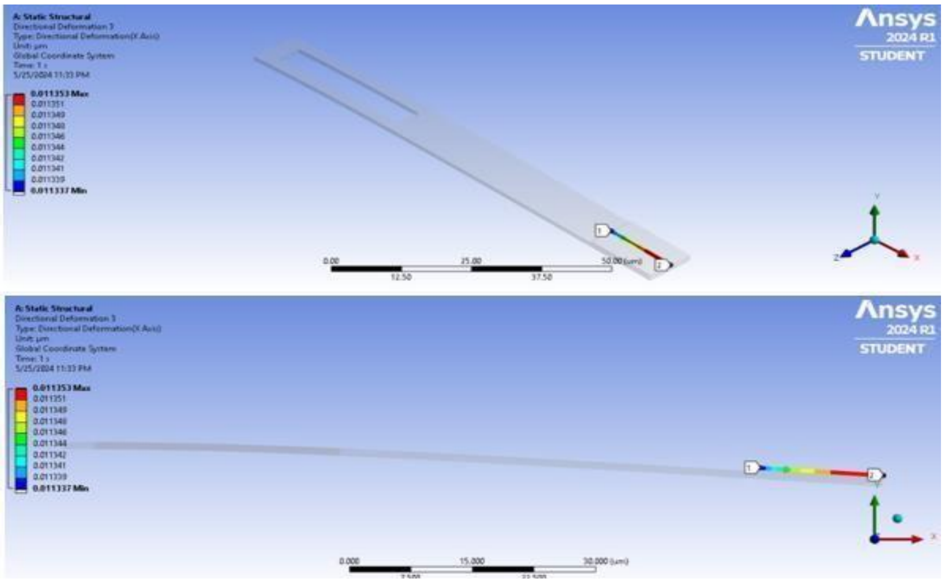

Figure 4.13: Equivalent stress plot along the sensing beam

The figures above represent the deformation pattern and stress distribution along the sensing beam with attached the graph plot of the equivalent stress. It results in maximum deflection at the starting edge of the sensing beam which is 0µm and as it moves along the sensing beam, the stress will be reduced, and so it can concluded that the load applied on the sensing beam basically mostly acting at the starting edge of the beam which means that the starting point will result in maximum sensitivity compared to other area of the beam.

4.6.2 Performance of cantilever with Square SCR

The performance of the microcantilever beam was simulated using ANSYS software with a rectangular SCR. The dimensions of this square hole will be 5x5µm. Figure 4.14 below shows the geometry imports to the model space for further analysis along with square SCR hole.

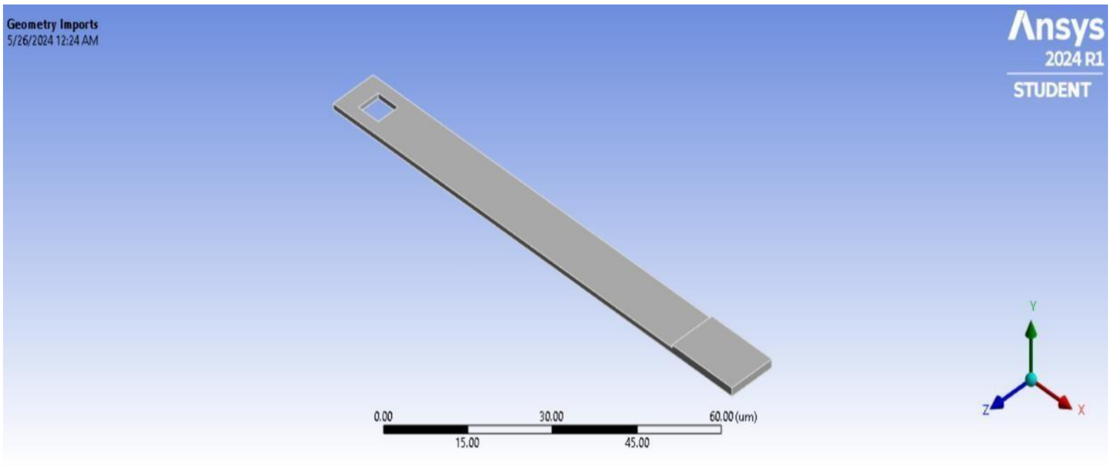

Figure 4.14: Geometry imports with square SCR

For Square Stress Concentration as shown in Figure 4.14 will having similar steps on carry out the analysis on the performance of the beam and hence the beam has been simulated through a range of force from 0.1 µN - 3 µN. Several parameters were observed and evaluated based on the presence of Stress Concentration Regions (SCR). A comparison will be made between the maximum deflection results of beams with and without SCR to determine if the SCR holes enhance the beam's sensitivity. The result then compared to previous study and look if the current designed has been improved with SCR added.

Table 4.6: Maximum result of cantilever beam with Square SCR

Force (µN)	Silicon Oxide		
	Maximum Deflection (µm)	Equivalent Stress (MPa)	Shear Stress (MPa)
0.1	0.605	13.297	1.0326
0.5	3.025	66.485	5.163
1	6.05	132.97	10.326
1.5	9.075	199.46	15.489
2	12.1	265.94	20.652
2.5	15.125	332.43	25.815
3	18.15	398.91	30.978

Table 4.6 above shows the simulation results for silicon oxide coated beam with a rectangular Stress Concentration Region. For 0.1 µN of force applied, the microcantilever beams record a maximum deflection of 0.605 µm and as the force keep increasing, the amount of deflection will be increase as well to a value of 18.15 µm when 3 µN load has applied on it. The result obtained in this section by using Square SCR will be slightly lower in terms of the maximum deflection compared to a rectangular stress concentration region.

There are several reasons that a square SCR doesn’t perform as well as a rectangular SCR. The first reason will be in terms of stress gradient, a rectangular SCR can help distribute stress more evenly across a larger area compared to a square SCR. This can reduce the intensity of stress concentration at any single point, leading to a lower likelihood of material failure. Next will be the factors of aspect ratio. The aspect ratio of a rectangular SCR allows for a more gradual transition of stress, which can help in minimizing peak stresses that typically occur at sharp corners in a square SCR.

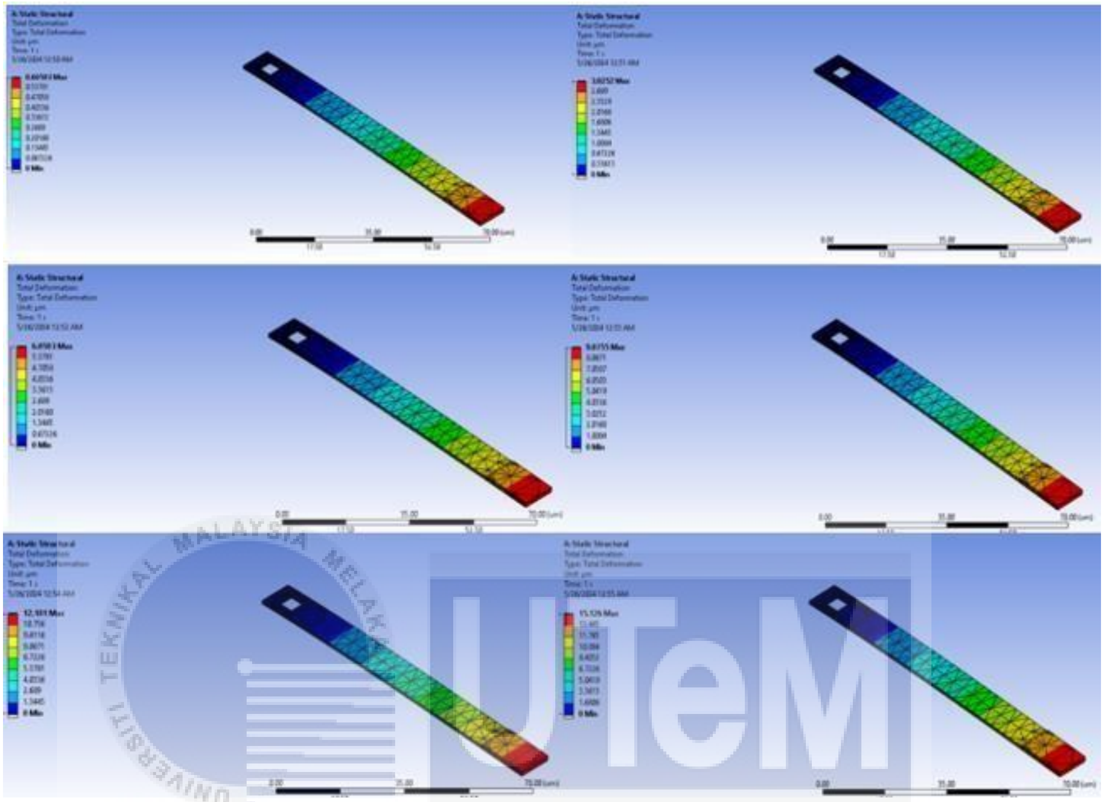

Figure 4.15: Maximum Deflection for Square SCR

Figure 4.15 above shows the deflection plot along with the stress distribution along the beam. The red colour area represents the maximum stress that acts on the beam which is the sensing area. The stress concentration region helps in distributing the load evenly compared to a normal beam. All these plots are based on a square Stress Concentration Region with dimensions of length = 0.5 µm and a width = 0.5 µm.

The deflection plot for the beam without square stress concentration region also having the same result as shown in Table 4.6 since the material using was the same for both beam and hence the maximum deflection will remain unchanged for a plain microcantilever beam without any SCR inserted.

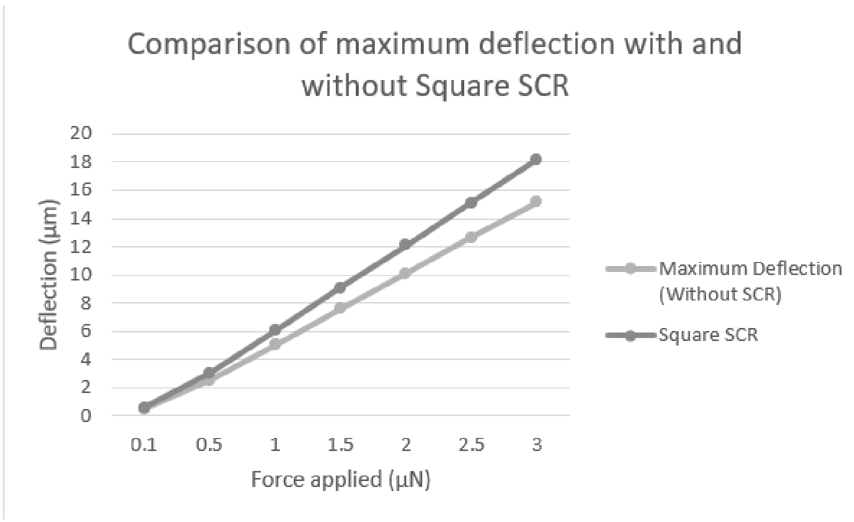

Figure 4.16: Graph of comparing performance of beam with and without Square SCR

Figure above represents the graph plot showing the results obtained from simulation according to the presence of SCR. It is notified that the deflection of the beam will still be higher with square SCR compared to the plain microcantilever beam. The improvement for square SCR will be slightly lower but it still increases the sensitivity of the microcantilever beam by resulting a higher maximum deflection.

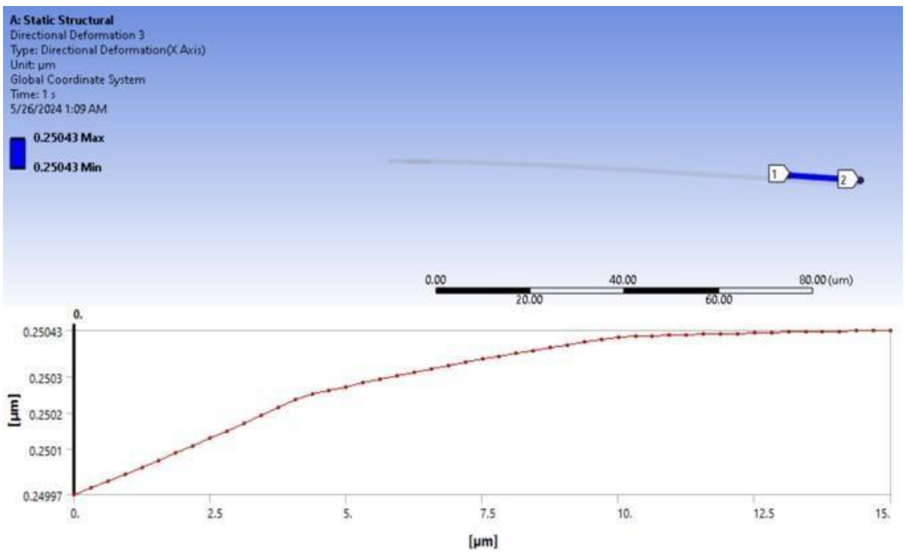

Figure 4.17: Directional Deformation along the sensing beam

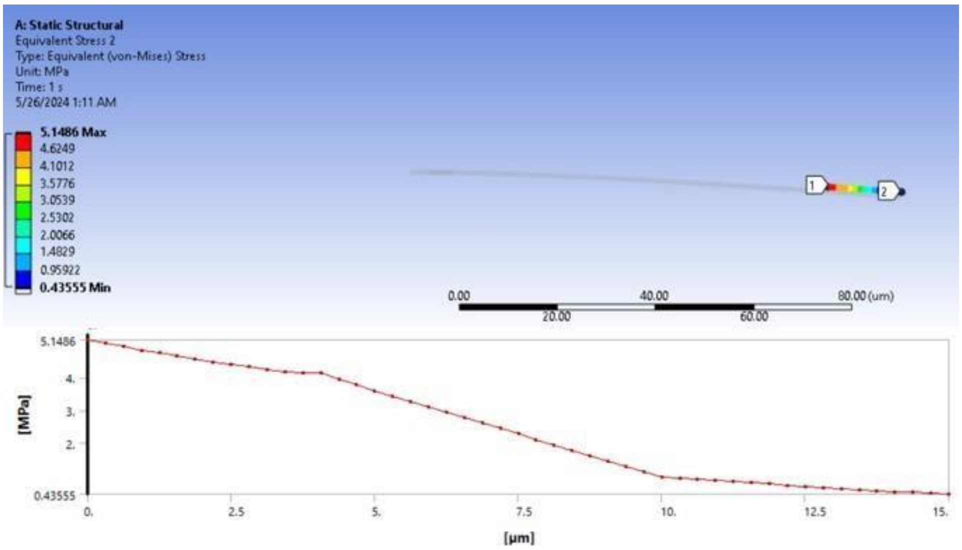

Figure 4.18: Equivalent stress plot along the sensing beam

The figures above show the deformation pattern and stress distribution along the sensing beam with attached the graph plot of the equivalent stress. It results in maximum deflection at the end of the edge of the sensing beam which is 15µm unlike the previous part of rectangular stress concentration region where the starting edge record the highest stress. In this section, the stress mostly acts on the ending edge of the beam by implementing a square stress concentration region hole.

4.6.3 Performance of cantilever with Circular SCR

The performance of the microcantilever beam was simulated using ANSYS software with a Circular SCR. The radius of this circular hole is 4µm and the distance is equal from the center of the surface of the beam which is 5 µm from center.

Figure 4.19 below shows the geometry imports to the model space for further analysis along with rectangular SCR hole.

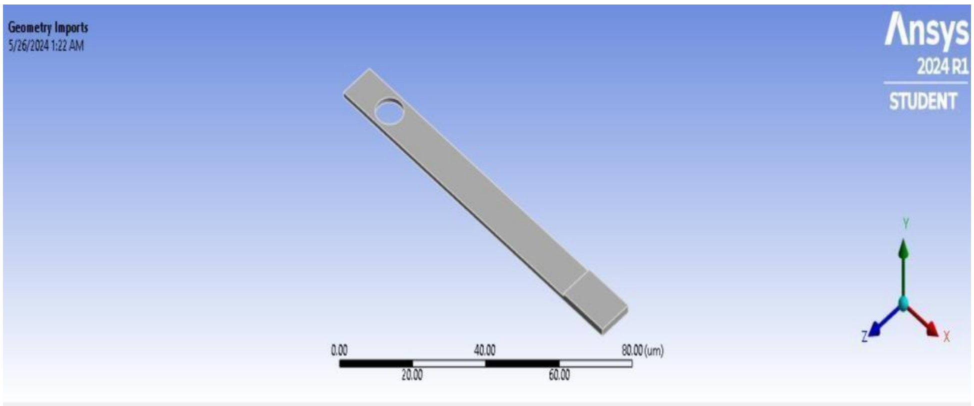

Figure 4.19: Geometry imports with circular SCR

For Circular Stress Concentration shown in figure above still conducting the exact steps but differ on designing the circular SCR. In this section, it is essential to ensure that the circular region is symmetry to the microcantilever beam to ensure the accuracy and sensitivity of the beam or else the distribution of load and stress will be uneven therefore will make changes on the maximum deflection. The analysis on the performance of the beam will be simulated through a range of force from 0.1 µN - 3 µN as previous study. Several parameters will be observed and evaluated based on the presence of Stress Concentration Regions (SCR).

Table 4.7: Maximum result of cantilever beam with Circular SCR

Force (μN)	Silicon Oxide		
	Maximum Deflection (μm)	Equivalent Stress (MPa)	Shear Stress (MPa)
0.1	0.7615	788.39	99.898
0.5	3.8075	3941.95	499.49
1	7.615	7883.9	998.98
1.5	11.423	11825.85	1498.47
2	15.23	15767.8	1997.96
2.5	19.0375	19709.75	2497.45
3	22.845	23651.7	2996.94

Table 4.7 above shows the simulation results for silicon oxide coated beam with a circular Stress Concentration Region. For 0.1 μN of force applied, the microcantilever beams record a maximum deflection of 0.7615 μm and as the force keep increasing, the amount of deflection will be increase as well to a value of 22.845 μm when 3 μN load has applied on it. The result obtained in this section by using Square SCR will be slightly lower in terms of the maximum deflection compared to a rectangular stress concentration region.

The reason that a circular Stress Concentration Region recorded a lower maximum deflection than rectangular SCR when same amount of load applied on the beam is because circular SCR will provide a less uniform stress distribution compared to rectangular SCR. The absence of sharp corners in a circular SCR minimizes the points of high stress concentration but leads to a less even spread of stress around the cutout. Moreover, an unsmooth stress flow will be one of the reasons it records a slightly lower maximum deflection than rectangular SCR. Even though Circular SCRs provide a smooth, continuous boundary than other SCR that allows stress to flow more evenly around the hole but the deflection of the beam with circular SCR still less than a rectangular SCR.

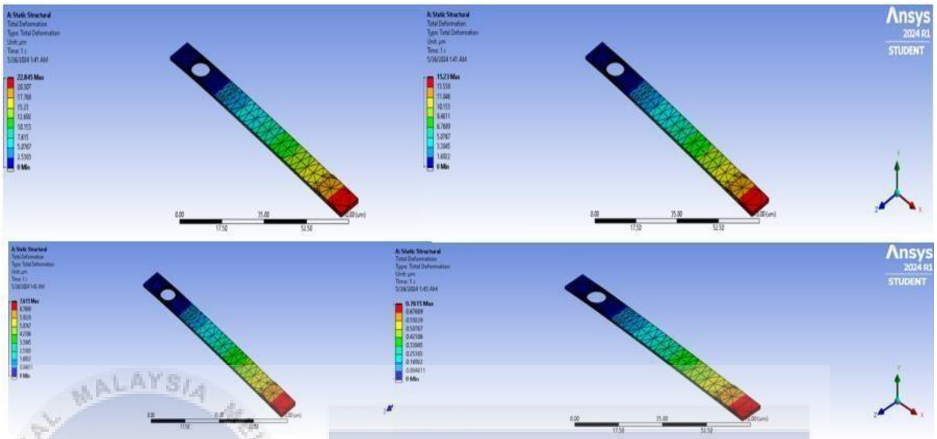

Figure 4.20: Maximum Deflection for Circular SCR

Figure 4.20 above shows the deflection plot along with the stress distribution along the beam. The red color in the plot indicates the areas of maximum stress on the beam, which is the critical sensing area. These observations are based on a circular SCR with a radius of 4μm. The stress concentration region (SCR) plays a crucial role in distributing the load more evenly compared to a beam without an SCR. By introducing an SCR, the beam can better manage and spread the applied stresses, reducing the likelihood of failure at any single point, and improving the overall performance and sensitivity of the beam.

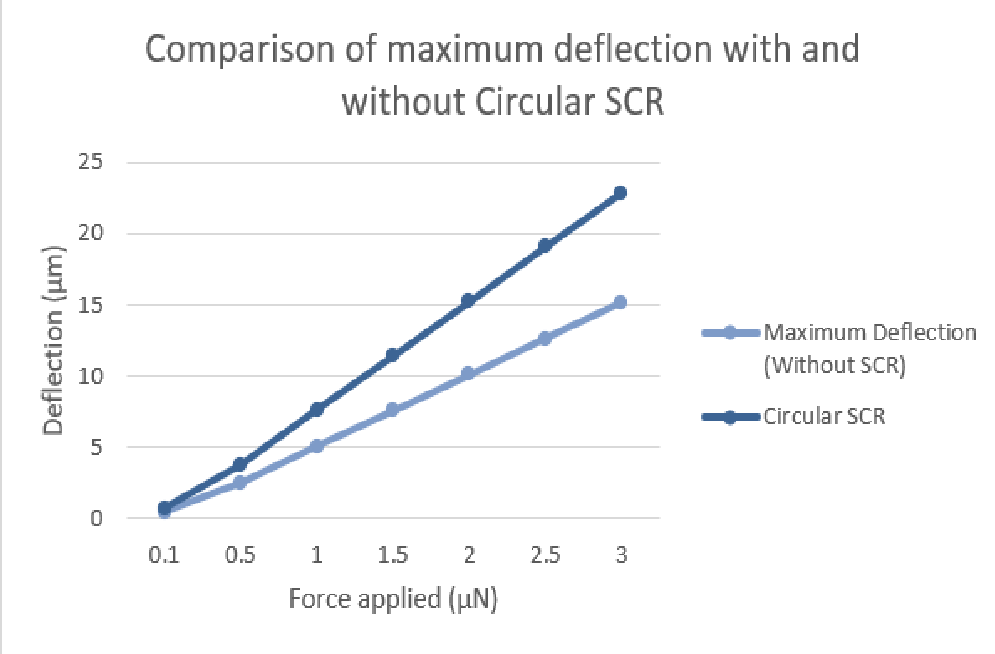

Figure 4.21: Graph of comparing performance of beam with and without Circular SCR

Figure above represents the graph plot showing the results obtained from simulation according to the presence of SCR. In this section by implementing the circular Stress Concentration Region, the maximum deflection is still higher than the microcantilever beam that doesn't insert the technique of SCR.

The maximum deflection on circular SCR beam will be slightly higher than rectangular SCR due to its numeric properties with smooth stress flow and lead to an even load stress distribution along the beam.

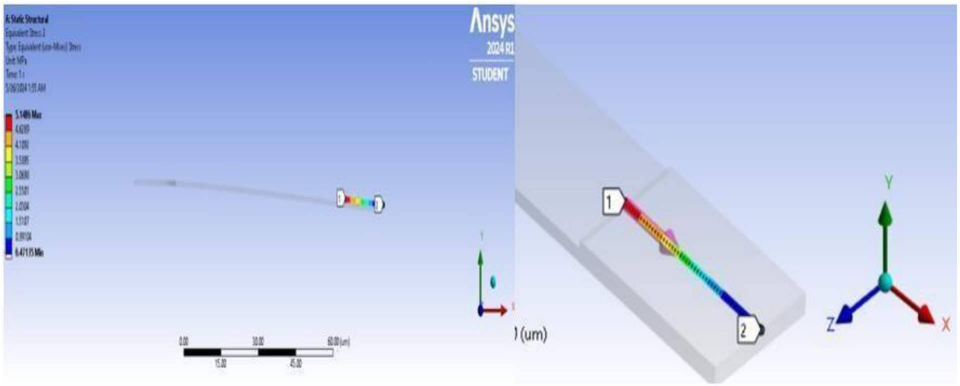

Figure 4.22: Stress distribution along the sensing beam

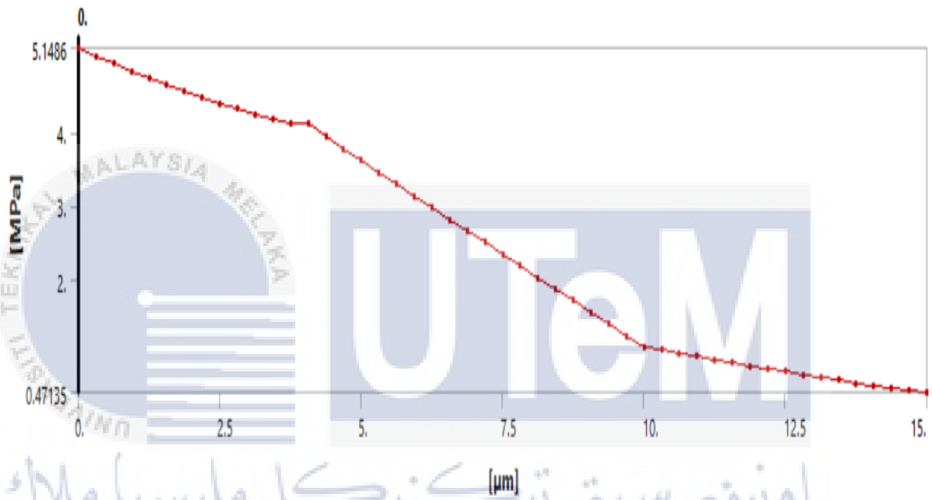

Figure 4.23: Equivalent stress plot along the sensing beam

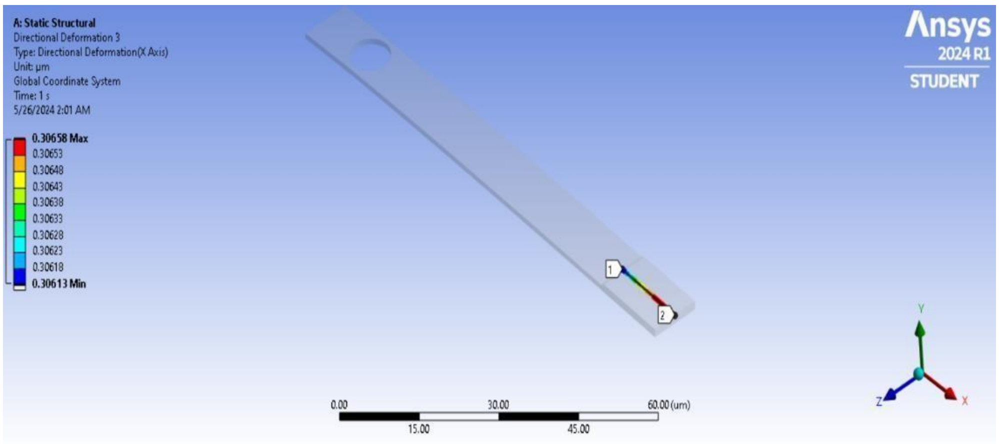

Figure 4.24: Total deformation shown along the sensing beam

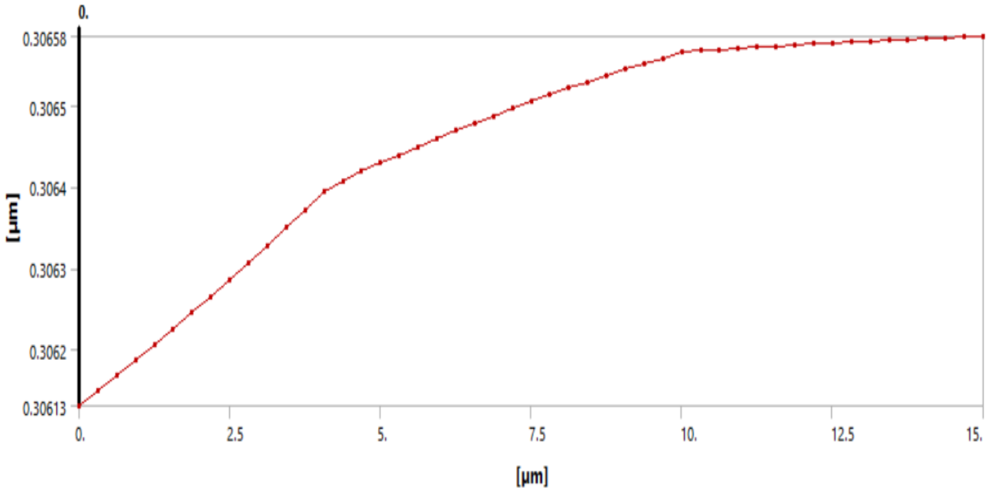

Figure 4.25: Maximum deflection plot along the sensing

The figures above show the deformation pattern and stress distribution along the sensing beam with attached the graph plot of the equivalent stress. In this stress concentration region, the deflection records the highest value at the end of the sensing beam whereas for the stress distribution it is vice versa, most of the stress will act on the starting edge of the beam compared to the ending edge.

This result could be crucial on determining which SCR is best suitable for sensing material as the force distribution and deflection area would be different and so to achieve a higher sensitivity, the effect on the position to the maximum displacement should be well study.

4.6.4 Performance of cantilever with Triangular SCR

The performance of the microcantilever beam was simulated using ANSYS software with a Triangular SCR. The triangular stress concentration region was built with a base width of 5µm and two symmetry line to the center of the cantilever beam.

Figure 4.26 below shows the geometry imports to the model space for further analysis along with triangular SCR hole.

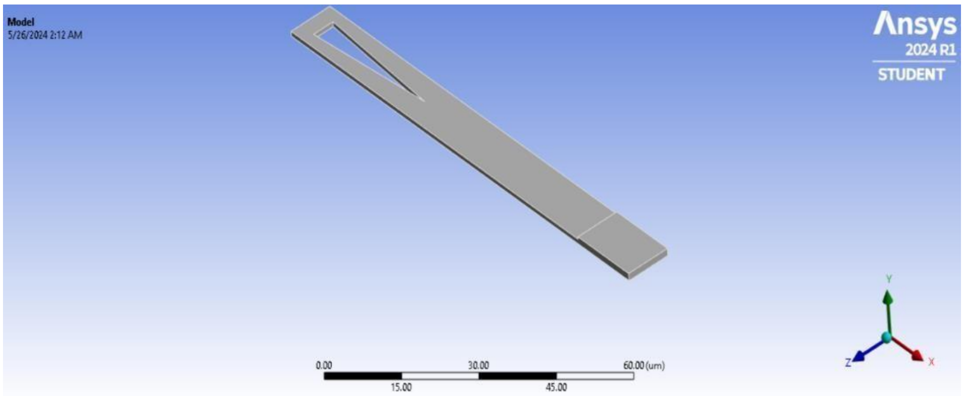

Figure 4.26: Geometry imports with triangular SCR

For Triangular Stress Concentration as shown in figure above will remain the same conducting steps but differ on designing using triangular SCR. In this section, the triangle is built with a base width of 5 µm which means that it placed at the center of the beam with a width of 10µm each side will remain an equal space of 2.5 µm for left and right to ensure that the pressure that act on the cantilever beam will be evenly distributed and result in maximum deflection. The analysis on the performance of the beam will be simulated through a range of force from 0.1 µN - 3 µN as previous study.

Several parameters will be observed and evaluated based on the presence of Stress Concentration Regions (SCR).

Table 4.8: Maximum result of cantilever beam with Triangular SCR

Force (μN)	Silicon Oxide		
	Maximum Deflection (μm)	Equivalent Stress (MPa)	Shear Stress (MPa)
0.1	0.6615	13.805	0.856
0.5	3.3077	69.025	4.279
1	6.6154	138.05	8.558
1.5	9.9231	207.075	12.837
2	13.2308	276.1	17.116
2.5	16.5385	345.125	21.395
3	19.846	414.15	25.674

Table 4.8 above shows the simulation results for silicon oxide coated beam with a Triangular Stress Concentration Region. For 0.1 μN of force applied, the microcantilever beams record a maximum deflection of 0.6615 μm and as the force keep increasing, the amount of deflection will be increase as well to a value of 19.846 μm when 3 μN load has applied on it. The result obtained in this section by using Triangular SCR will be slightly lower than Circular and Rectangular SCR but higher than square SCR in terms of the maximum deflection.

The reason that a Triangular Stress Concentration Region recorded a lower maximum deflection than rectangular SCR when same amount of load applied on the beam is because of its sharp corners. The sharp corners present in triangular SCR which serve as points of significant stress concentration. However, these corners are more acute compared to those in triangular SCRs, resulting in even higher stress peaks.

But then it records lower deflection compared to circular beam since circular SCR provides a more uniform stress distribution around their edges, minimizing localized peaks and allowing for greater overall deflection.

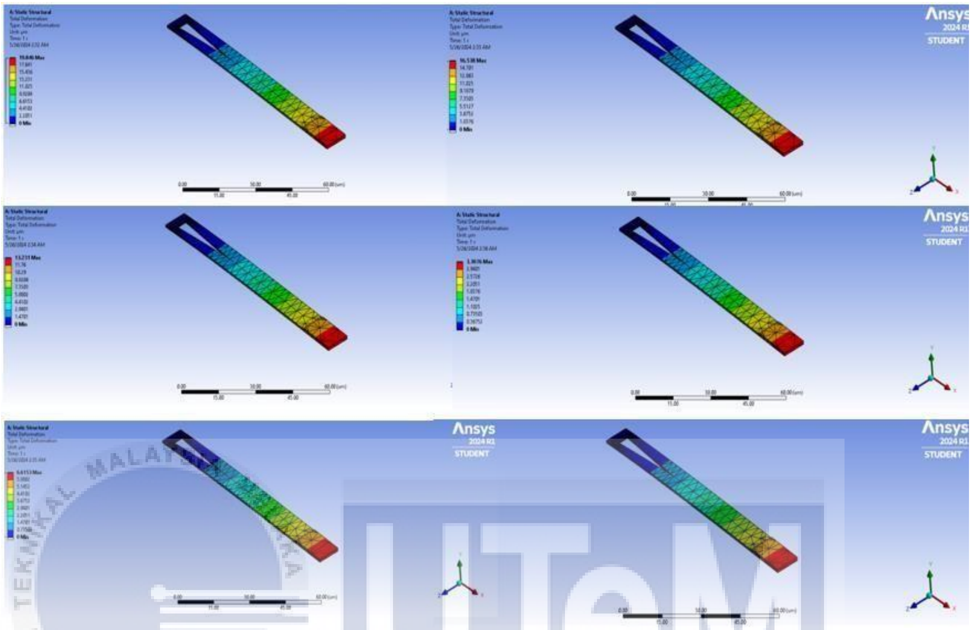

Figure 4.27: Maximum Deflection for Triangular SCR

Figure 4.27 above shows the deflection plot along with the stress distribution along the beam. The red color in the plot indicates the areas of maximum stress on the beam, which is the critical sensing area. These observations are based on a triangular SCR with a base width of 5µm and the symmetry line of 30 µm to the center of the beam. The Stress Concentration Region (SCR) plays a crucial role in distributing the load more evenly compared to a beam without an SCR. By introducing an SCR, the beam can better manage and spread the applied stresses, reducing the likelihood of failure at any single point. This improved stress management enhances the overall performance and sensitivity of the beam, making it more effective in its applications.

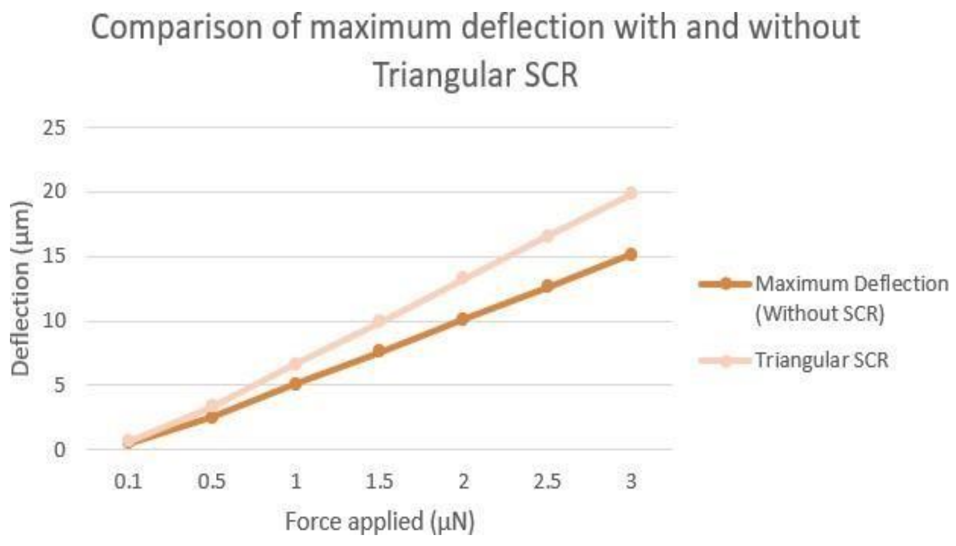

Figure 4.28: Graph of comparing performance of beam with and without Triangular SCR

Figure 4.28 represents the graph plot showing the results obtained from simulation according to the presence of SCR. In this section by implementing the Triangular Stress Concentration Region, the maximum deflection is still higher than the microcantilever beam that doesn't insert the technique of SCR. The maximum deflection on triangular SCR beam will be slightly higher than rectangular SCR due to the properties of sharp corners and stress gradients. Basically, this Stress concentration region can increase and improve the sensitivity of the pure cantilever beam and make it more reliable due to its responsiveness to the load that is applied on it.

Figure 4.29: Stress distribution along the sensing beam

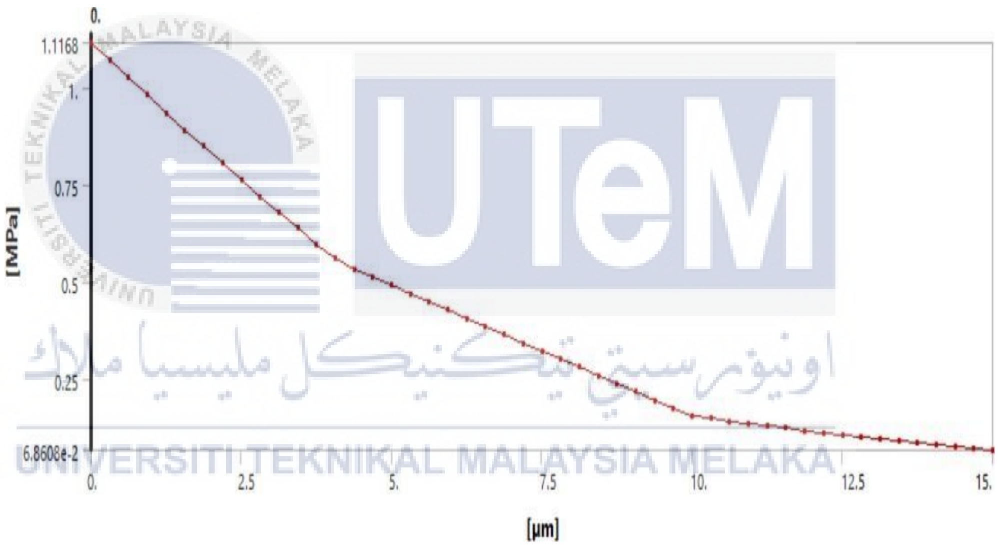

Figure 4.30: Equivalent stress plot along the sensing beam

The figures above represent the equivalent stress plot for the cantilever beam with triangular Stress Concentration Region. For this part, the stress is mainly focused on the starting edge of the sensing beam and decreases proportionally when it moves along the beam.

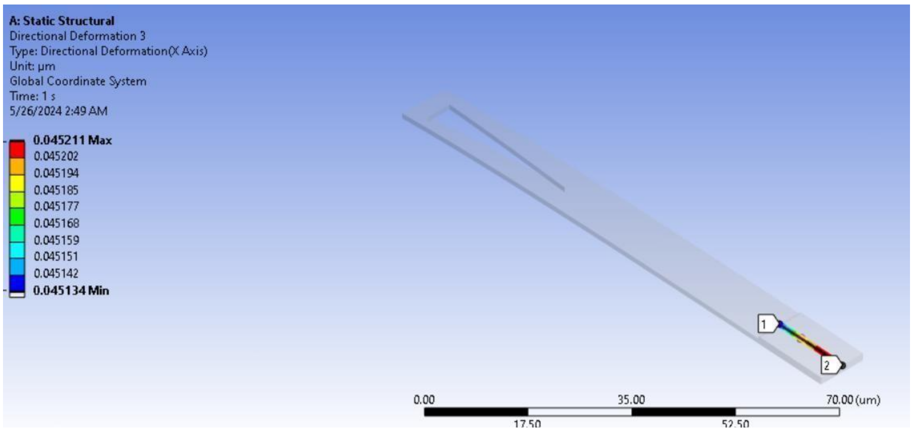

Figure 4.31: Total deformation shown along the sensing beam

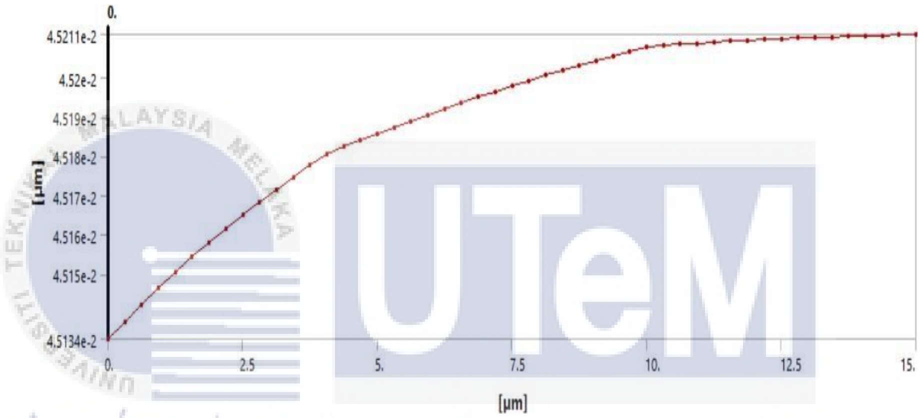

Figure 4.32: Maximum deflection plot along the sensing beam

Figure 4.31 and Figure 4.32 show the total deformation of the beam where the red area will explain about which part of the beam will observe a maximum deflection when a load is applied on it and this result shows that at the ending edge of the beam will have the highest deflection compared to others part of the beam.

4.7 Comparison of deflection with various SCR & without SCR

After computing different types of Stress Concentration Region including Rectangular, Square, Circular and Triangular, it is essential for us to find out which designed give the best sensitivity as it records the highest deflection among all.

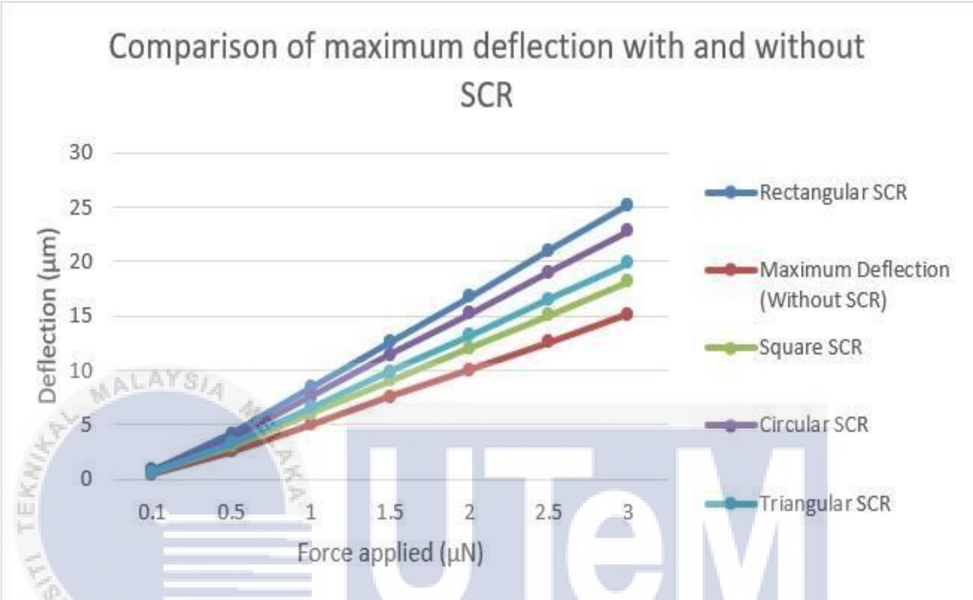

Figure 4.33: Comparison of various SCR with a plain cantilever beam

From the figure above it is clearly seen that the microcantilever beam can perform better with attaching a stress concentration region hole compared to an original beam. Based on the graph that has been plotted, rectangular SCR records the maximum deflection followed by circular SCR, Triangular SCR, Square SCR and finally the beam without any SCR.

Therefore, it can conclude that Rectangular Stress Concentration Region is most suitable for designing a Microcantilever beam with Silicon Oxide material as the sensing material. These combinations result in the highest sensitivity compared to others and will result in more accurate result data.

4.8 Relationship between length of Rectangular SCR with maximum deflection

After the completion of determining the most suitable Stress Concentration Region that gives the maximum deflection among 4 SCR which represented by the Rectangular SCR. It is important to know how the beam performs if the parameters of the rectangular stress concentration are changed by varying the length of the rectangular stress concentration.

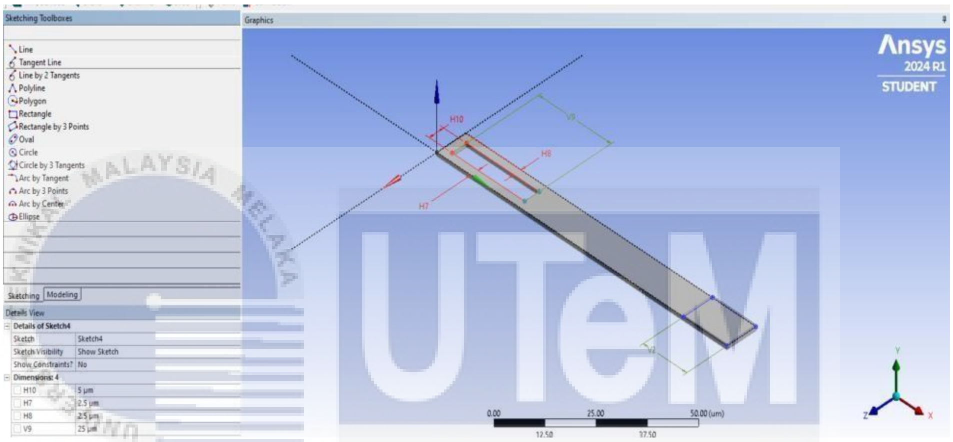

Figure 4.34: Rectangular SCR with varying length

Figure above shows the model of the microcantilever with rectangular stress concentration region. The length of the rectangular SCR has been varying as the initial length represents by 30µm and to determine the effect on the beam performance in terms of maximum deflection to observed whether the performance will be increased or decreased. There are total of 5 different lengths tested and simulated which are 30 µm, 25µm, 20µm, 15µm and 10µm. The performance of the beam was tabulated as shown in Table 4.9 below. All the simulation are done with a force applied of 0.1µN to indicate the relationship of these 2 parameters.

Table 4.9: Performance comparison by varying length of rectangular SCR

Force applied (μN)	Length of Rectangular SCR (μm)	Maximum deflection (μm)
0.1	30	0.8407
	25	0.7178
	20	0.6802
	15	0.6378
	10	0.5910

Table 4.9 above shows that the maximum deflection of the microcantilever beam decreased as the length of the rectangular stress concentration region decreased. This is due to the force distribution of the beam not being evenly and the structural stiffness increased as the beam deflected less under the same load and force applied. Furthermore, the length of the beam will be directly proportional to the maximum deflection. Therefore, it can be concluded that the length of Rectangular SCR which give the best performance among 4 types of SCR is 30μm and the maximum deflection decreased as the length of SCR decreased.

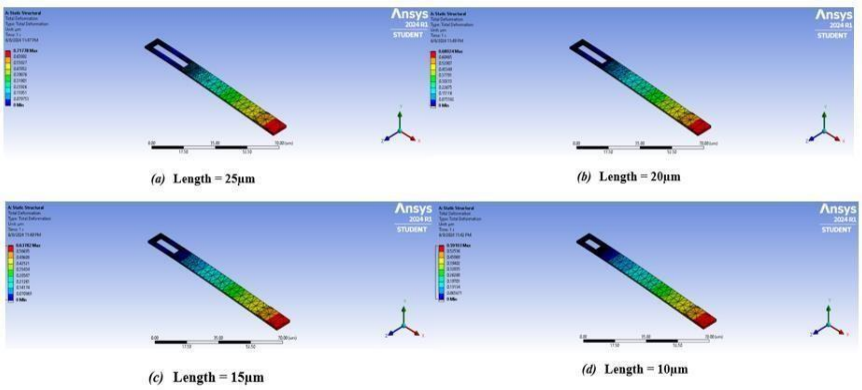

Figure 4.35: Simulation on different length of Rectangular SCR

Figure above shows that the simulation on the maximum deflection of the microcantilever beam by varying the length of rectangular Stress Concentration Region into 4 different levels. After the results have been tabulated, it is then crucial to analyze the relationship between the length of stress concentration region with maximum deflection by plotting a graph as shown in Figure 4.36 below.

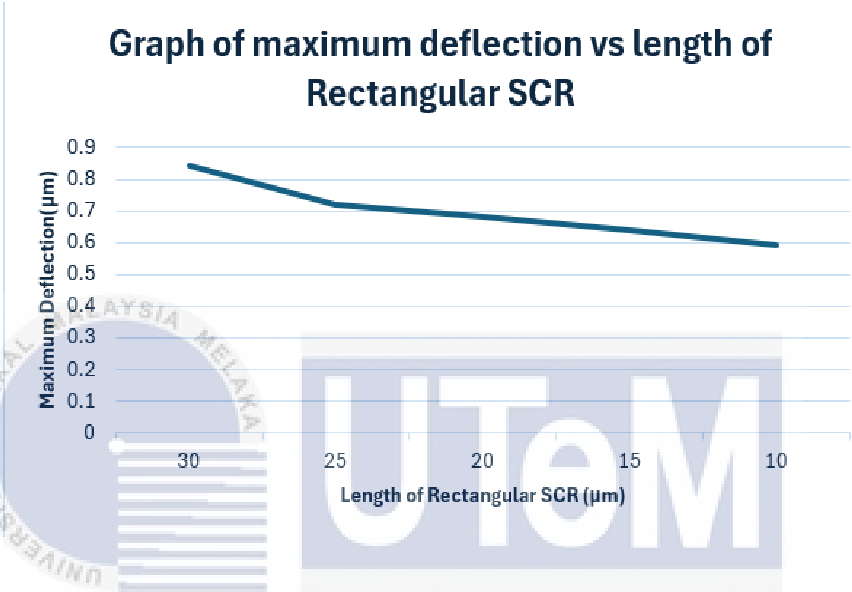

Figure 4.36: Graph of maximum deflection vs various length of rectangular SCR

As the results shown in Figure 4.36 concluded that the length of rectangular Stress Concentration Region is directly related to the maximum deflection hence the deflection reduced as the length reduced.

4.9 Performance comparison with previous study

According to the research done by Dinesh Rotake (2018), a microcantilever beam with stress concentration region can improve overall performance and the simulation was done using various types of SCR as similar in this thesis.

Therefore, the performance based on the maximum deflection of the cantilever beam using different SCR was compared and tabulated as shown in Table 4.10 below to investigate whether this design has improved the sensitivity compared to others.

Table 4.10: Performance comparison on the beam deflection

Types of SCR	Previous study (μm) Dinesh Rotake (2018)	**Current study (μm)**	Percentage improvement (%)
Rectangular	15.2	**21.1**	27.96
Circular	12.1	**19.0**	36.32
Square	12.2	**15.1**	19.20
Triangular	11.9	**16.5**	27.88

Based on Table 4.10 above, it can be concluded that both studies agreed on the rectangular Stress Concentration Region give result in maximum deflection compared to other SCRs and the beam without any SCRs. All the result are based on a force of 2.5μN. The result will be affected by various parameters such as the dimension of the beam, material used for sensing, material sized for meshing would all result in different simulation result. The percentage of improvement is around 27% on average and so this design results in better sensitivity due to its higher maximum deflection.

CHAPTER 5

CONCLUSION AND FUTURE WORKS

The purpose of this paper is to design a microcantilever beam for portable heavy metal ion detections and hence it is essential to analyze the performance of the cantilever beam in terms of the maximum deflection which will be directly reflected to the sensitivity of the beam. Therefore, 2 different software has been implemented in this paper which are COMSOL Multiphysics and ANSYS Workbench. First, COMSOL software was used to identify the best dimensions of the beam along with the most suitable sensing materials. Next, the geometry was transformed to ANSYS Workbench for further FEA analysis using different types of SCRs.

The ANSYS software package was utilized to model the mechanical behavior of silicon-based cantilevers. The study investigated the integration of Stress Concentration Regions (SCRs) with a thickness less than that of the cantilever to localize stresses and improve maximum displacement and force sensitivities. Additionally, the design of cantilevers with reduced width was explored, focusing on four basic shapes: rectangular, circular, square, and triangular.

It was observed that the placement of the SCR was crucial. Optimal placement and thickness of the cantilever were found to significantly enhance maximum beam displacement, force, and stress sensitivities. These results underscore the importance of SCR design in optimizing the performance of silicon-based cantilevers for sensing applications. In short, the result obtained as shown above concluded that rectangular SCRs will provide the best sensitivity as it gives out the highest maximumdeflection and this paper has proposed a design which shows an improvement

compared to previous studies. The design parameters for this paper are 100x10x1μm for cantilever beam dimensions and Silicon Oxide as the most suitable sensing materials.

5.1 Future Works

The designed parameters can be further improved by observing other materials that have elastic properties better than Silicon Oxide. Moreover, the fabrication of the capacitive sensor along with the microfluidic platform will also be the focus point on developing a portable Heavy Metal Ion Detector.

REFERENCES

[1] S. C. Wilschefski and M. R. Baxter, "Inductively Coupled Plasma Mass Spectrometry: Introduction to Analytical Aspects," *Clinical Biochemist Reviews*, vol. 40, no. 3, pp. 115–133, Aug. 2019, doi: https://doi.org/10.33176/aacb-19-00024.

[2] Varnakavi. Naresh and N. Lee, "A Review on Biosensors and Recent Development of Nanostructured Materials-Enabled Biosensors," *Sensors*, vol. 21, no. 4, p. 1109, Feb. 2021, doi: https://doi.org/10.3390/s21041109.

[3] S. 1, P. Jm, and P. Deep, "DESIGN of MICRO CANTILEVER BEAM for VAPOUR DETECTION USING COMSOL MULTI PHYSICS SOFTWARE." Accessed: Jan. 07, 2024. [Online]. Available: https://www.enggjournals.com/ijet/docs/IJET15-07-03-312.pdf

[4] P. B. Tchounwou, C. G. Yedjou, A. K. Patlolla, and D. J. Sutton, "Heavy Metal Toxicity and the Environment," *Experientia Supplementum*, vol. 101, no. 1, pp. 133–164, Aug. 2014, doi: https://doi.org/10.1007/978-3-7643-8340-4_6.

[5] M.-R. Ghazavi, G. Rezazadeh, and S. Azizi, "Pure parametric excitation of a micro cantilever beam actuated by piezoelectric layers," *Applied Mathematical Modelling*, vol. 34, no. 12, pp. 4196–4207, Dec. 2010, doi: https://doi.org/10.1016/j.apm.2010.04.017.

[6] T. Hu, Q. Lai, W. Fan, Y. Zhang, and Z. Liu, "Advances in Portable Heavy Metal Ion Sensors," Sensors, vol. 23, no. 8, pp. 4125–4125, Apr. 2023, doi: https://doi.org/10.3390/s23084125.

[7] S. Srivastava and V. Sharma, "Ultra-portable, smartphone-based spectrometer for heavy metal concentration measurement in drinking water samples," Applied Water Science, vol. 11, no. 11, Oct. 2021, doi: https://doi.org/10.1007/s13201-021-01519-w.

[8] Hiang Kwee Lee et.al., "Sensitive, portable heavy-metal-ion detection by the sulfidation method on a superhydrophobic concentrator (SPOT)," vol. 4, no. 5, pp. 756–766, May 2021, doi: https://doi.org/10.1016/j.oneear.2021.04.009.

[9] B. Unnikrishnan, C.-W. Lien, H.-W. Chu, and C.-C. Huang, "A review on metal nanozyme-based sensing of heavy metal ions: Challenges and future perspectives," Journal of Hazardous Materials, vol. 401, p. 123397, Jan. 2021, doi: https://doi.org/10.1016/j.jhazmat.2020.123397.

[10] D. Rotake and A. D. Darji, "Heavy Metal Ion Detection in Water using MEMS Based Sensor," Materials Today: Proceedings, vol. 5, no. 1, pp. 1530–1536, 2018, doi: https://doi.org/10.1016/j.matpr.2017.11.242.

[11] S. Cherian, "Detection of heavy metal ions using protein-functionalized microcantilever sensors," Biosensors and Bioelectronics, vol. 19, no. 5, pp. 411–416, Dec. 2003, doi: https://doi.org/10.1016/s0956-5663(03)00226-4.

[12] H. Ji, "In situ detection of calcium ions with chemically modified microcantilevers," Biosensors and Bioelectronics, vol. 17, no. 4, pp. 337–343, Apr. 2002, doi: https://doi.org/10.1016/s0956-5663(01)00270-6.

[13] W. J. Venstra, W. H. Wien, P. M. Sarro, and J. van Eijk, "Microcantilevers encapsulated in fluid wells for sensing in liquids," Microelectronic Engineering, vol. 97, pp. 247–250, Sep. 2012, doi: https://doi.org/10.1016/j.mee.2012.03.030.

[14] W. Xiang and C. Lee, "Nanophotonics Sensor Based on Microcantilever for Chemical Analysis," IEEE Journal of Selected Topics in Quantum Electronics, vol. 15, no. 5, pp. 1323–1326, Jan. 2009, doi: https://doi.org/10.1109/jstqe.2009.2016578.

[15] Nur Hasiba Kamaruddin, Nur, Nurul Fariha Lokman, and A. Ashrif, "Effect of bimetallic structure on the performance of chitosan-graphene oxide surface plasmon resonance sensor," Sep. 2014, doi: https://doi.org/10.1109/icp.2014.7002350.

[16] B. Wang, F. Huang, T. Nguyen, and Q. Lin, "Microcantilever-based label-free thermal characterization of biomolecular affinity binding," Jan. 2010, doi: https://doi.org/10.1109/memsys.2010.5442341.

[17] J. Feng, X. Ye, Y. Shang, K. Wu, and F. Chen, “ Integrated dual - grating inteferometric detection with polymer microbeams for bio-chemical sensing in liquid environment,” Micro & Nano Letters, vol. 8, no. 10, pp. 629–632, Oct. 2013, doi: https://doi.org/10.1049/mnl.2013.0237.

[18] Hans Peter Lang, F. Huber, J. Zhang, and C. Gerber, “MEMS technologies in life sciences,” Jun. 2013, doi: https://doi.org/10.1109/transducers.2013.6626686.

[19] M. Chaudhary and A. Gupta, “Microcantilever-based Sensors,” Defence Science Journal, vol. 59, no. 6, pp. 634–641, Nov. 2009, doi: https://doi.org/10.14429/dsj.59.1569.

[20] S. M. Firdaus, I. A. Azid, O. Sidek, K. Ibrahim, and M. Hussien, “Enhancing the sensitivity of a mass-based piezoresistive micro-electro-mechanical systems cantilever sensor,” Micro & Nano Letters, vol. 5, no. 2, p. 85, 2010, doi: https://doi.org/10.1049/mnl.2009.0105.

[21] M. Asghar Bhatti, Lee Chang Xi, Lee Yue Zhong, and A. N. Abdalla, “Design and Finite Element Analysis of Piezoresistive Cantilever with Stress Concentration Holes,” May 2007, doi: https://doi.org/10.1109/iciea.2007.4318591.

[22] S. Sang, Y. Zhao, W. Zhang, P. Li, J. Hu, and G. Li, “Surface stress-based biosensors,” Biosensors and Bioelectronics, vol. 51, pp. 124–135, Jan. 2014, doi: https://doi.org/10.1016/j.bios.2013.07.033.

[23] B. Bansod, T. Kumar, R. Thakur, S. Rana, and I. Singh, "A review on various electrochemical techniques for heavy metal ions detection with different sensing platforms," Biosensors and Bioelectronics, vol. 94, pp. 443–455, Aug. 2017, doi: https://doi.org/10.1016/j.bios.2017.03.031.

[24] G. Tsekenis, M. K. Filippidou, M. Chatzipetrou, V. Tsouti, I. Zergioti, and S. Chatzandroulis, "Heavy metal ion detection using a capacitive micromechanical biosensor array for environmental monitoring," Sensors and Actuators B: Chemical, vol. 208, pp. 628– 635, Mar. 2015, doi: https://doi.org/10.1016/j.snb.2014.10.093

[25] S. Arora, "Design Of Mems Based Microcantilever Using Comsol Multiphysics," *Research India Publications;*, Available: https://www.academia.edu/3066170/Design_Of_Mems_Based_Microcantilever_Using_Comsol_Multiphysics

[26] Y. Liu, X. Jiang, H. Yang, H. Qin, and W. Wang, "Structural Engineering in Piezoresistive Micropressure Sensors: A Focused Review," *Micromachines*, vol. 14, no. 8, p. 1507, Aug. 2023, doi: https://doi.org/10.3390/mi14081507.

[27] R. Zhao and Y. Sun, "Polymeric Flexible Immunosensor Based on Piezoresistive Micro-Cantilever with PEDOT/PSS Conductive Layer," *Sensors*, vol. 18, no. 2, p. 451, Feb. 2018, doi: https://doi.org/10.3390/s18020451.

[28] S. 1, P. Jm, and P. Deep, "DESIGN of MICRO CANTILEVER BEAM for VAPOUR DETECTION USING COMSOL MULTI PHYSICS SOFTWARE." Accessed: Jan. 07, 2024. [Online]. Available: https://www.enggjournals.com/ijet/docs/IJET15-07-03-312.pdf

[29] G. Zhao *et al.*, "Multiplexed Anodic Stripping Voltammetry Detection of Heavy Metals in Water Using Nanocomposites Modified Screen-Printed Electrodes Integrated With a 3D-Printed Flow Cell," *Frontiers in Chemistry*, vol. 10, p. 815805, Feb. 2022, doi: https://doi.org/10.3389/fchem.2022.815805.

[30] D. Grieshaber, R. MacKenzie, J. Vörös, and E. Reimhult, "Electrochemical Biosensors - Sensor Principles and Architectures," *Sensors*, vol. 8, no. 3, pp. 1400–1458, Mar. 2008, doi: https://doi.org/10.3390/s80314000.

[31] V. K. Gupta, "Potentiometric Sensors for Heavy Metals – An Overview," *CHIMIA International Journal for Chemistry*, vol. 59, no. 5, pp. 209–217, May 2005, doi: https://doi.org/10.2533/000942905777676614.

[32] M. G. G. Jithendra Prasad and S. Syed, "Design and analysis of Micro-Cantilever based Biosensor for Swine flu Detection," *International Journal of Electrical and Computer Engineering (IJECE)*, vol. 6, no. 3, p. 1190, Jun. 2016, doi: https://doi.org/10.11591/ijece.v6i3.pp1190-1196.

APPENDICES

Appendix A: Weight Distribution for Different Heavy Metal Ions

METAL IONS	ATOMIC MASS UNIT (AMU)	WEIGHT (gram/mol)
Lead(Pb^{2+})	207.2	207.2
Mercury(Hg^{2+})	200.6	200.6
Cadmium(Cd^{2+})	112.4	112.4
Copper(Cu^{2+})	63.5	63.5
Iron(Fe^{2+})	55.8	55.8
Zinc(Zn^{2+})	65.4	65.4
Silver(Ag^{+})	107.9	107.9
Gold(Au^{2+})	196.9	196.9
Platinum(Pt^{2+})	195.1	195.1
Nickel(Ni^{2+})	58.7	58.7
Manganese(Mn^{2+})	54.9	54.9
Chromium(Cr^{3+})	51.9	51.9
Cobalt(Co^{2+})	58.9	58.9
Tin(Sn^{2+})	118.7	118.7
Bismuth(Bi^{3+})	208.9	208.9

Appendix B: EPA Permissible limit for various Heavy Metal Ion

METAL IONS	EPA Limit ($\mu g L^{-1}$)
Lead(Pb^{2+})	15
Mercury(Hg^{2+})	2
Cadmium(Cd^{2+})	5
Copper(Cu^{2+})	1.3
Iron(Fe^{2+})	15
Zinc(Zn^{2+})	5
Nickel(Ni^{2+})	100
Arsenic(As^{3+})	10
Chromium(Cr^{3+})	100
Selenium(Se^{4+})	50
Uranium(U^{5+})	30
Antimony(Sb^{3+})	6

Appendix C: EU Permissible limit for various Heavy Metal Ion

METAL IONS	**EPA Limit ($\mu g L^{-1}$)**
Lead(Pb^{2+})	10
Mercury(Hg^{2+})	1
Cadmium(Cd^{2+})	5
Copper(Cu^{2+})	2
Iron(Fe^{2+})	10
Zinc(Zn^{2+})	5
Nickel(Ni^{2+})	20
Arsenic(As^{3+})	10
Chromium(Cr^{3+})	50
Selenium(Se^{4+})	40
Uranium(U^{5+})	30
Antimony(Sb^{3+})	5

Appendix D: WHO Permissible limit for various Heavy Metal Ion

METAL IONS	**EPA Limit ($\mu g L^{-1}$)**
Lead(Pb^{2+})	10
Mercury(Hg^{2+})	6
Cadmium(Cd^{2+})	3
Copper(Cu^{2+})	2
Iron(Fe^{2+})	5
Zinc(Zn^{2+})	5
Nickel(Ni^{2+})	20
Arsenic(As^{3+})	10
Chromium(Cr^{3+})	25
Selenium(Se^{4+})	10
Uranium(U^{5+})	30
Antimony(Sb^{3+})	5

Appendix E: Summary Simulation Data in ANSYS

Project*

First Saved	Thursday, May 2, 2024
Last Saved	Monday, June 10, 2024
Product Version	2024 R1
Save Project Before Solution	No
Save Project After Solution	No

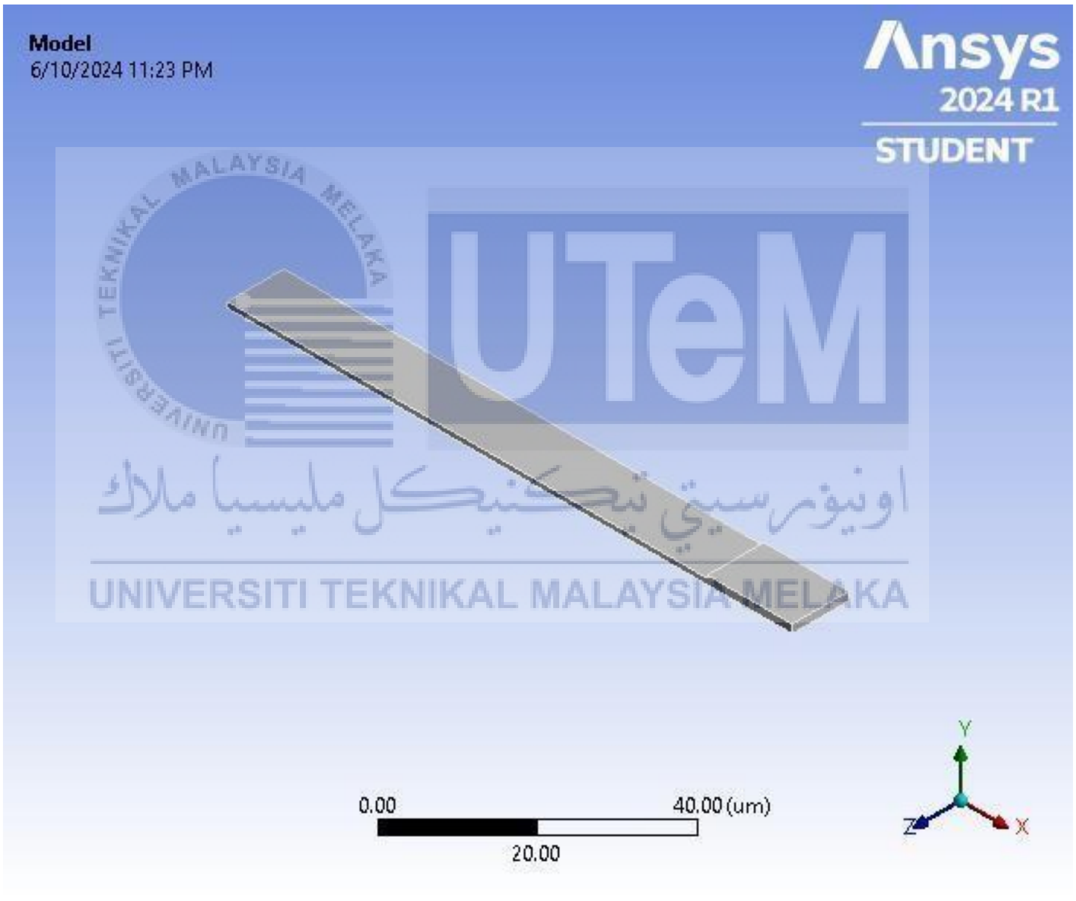

Contents

Units

TABLE 1

Unit System	Metric (µm, kg, µN, s, V, mA) Degrees rad/s Celsius
Angle	Degrees
Rotational Velocity	rad/s
Temperature	Celsius

Model (A4)

TABLE 2
Model (A4) > Geometry Imports

Object Name	*Geometry Imports*
State	Solved

TABLE 3
Model (A4) > Geometry Imports > Geometry Import (A3)

Object Name	*Geometry Import (A3)*
State	Solved
Definition	
Source	C:\Users\Acer\Desktop\gold_files\dp0\SYS\DM\SYS.agdb
Type	DesignModeler
Basic Geometry Options	
Parameters	Independent
Parameter Key	
Advanced Geometry Options	
Compare Parts On Update	No
Analysis Type	3-D

Geometry

TABLE 4
Model (A4) > Geometry

Object Name	*Geometry*
State	Fully Defined
Definition	
Source	C:\Users\Acer\Desktop\gold_files\dp0\SYS\DM\SYS.agdb
Type	DesignModeler
Length Unit	Micrometers
Element Control	Program Controlled
Display Style	Body Color
Bounding Box	
Length X	100. µm
Length Y	1.5 µm
Length Z	10. µm
Properties	
Volume	1075. µm³
Mass	0. kg
Scale Factor Value	1.
Statistics	
Bodies	1
Active Bodies	1
Nodes	877
Elements	96
Mesh Metric	None
Update Options	
Assign Default Material	No
Basic Geometry Options	
Parameters	Independent
Parameter Key	
Attributes	Yes
Attribute Key	
Named Selections	Yes
Named Selection Key	
Material Properties	Yes
Advanced Geometry Options	
Use Associativity	Yes
Coordinate Systems	Yes
Coordinate System Key	
Reader Mode Saves Updated File	No
Use Instances	Yes
Smart CAD Update	Yes
Compare Parts On Update	No
Analysis Type	3-D
Import Facet Quality	Source
Clean Bodies On Import	No
Stitch Surfaces On Import	None
Decompose Disjoint Geometry	Yes
Enclosure and Symmetry Processing	Yes

TABLE 5
Model (A4) > Geometry > Parts

Object Name	*Solid*
State	Meshed

Graphics Properties	
Visible	Yes
Transparency	1
Definition	
Suppressed	No
Stiffness Behavior	Flexible
Coordinate System	Default Coordinate System
Reference Temperature	By Environment
Treatment	None
Material	
Assignment	Gold
Nonlinear Effects	Yes
Thermal Strain Effects	Yes
Bounding Box	
Length X	100. µm
Length Y	1.5 µm
Length Z	10. µm
Properties	
Volume	1075. µm³
Mass	0. kg
Centroid X	35.069 µm
Centroid Y	-4.3477 µm
Centroid Z	5. µm
Moment of Inertia Ip1	0. kg·µm²
Moment of Inertia Ip2	0. kg·µm²
Moment of Inertia Ip3	0. kg·µm²
Statistics	
Nodes	877
Elements	96
Mesh Metric	None

TABLE 6
Model (A4) > Materials

Object Name	*Materials*
State	Fully Defined
Statistics	
Materials	2
Material Assignments	0

Coordinate Systems

TABLE 7
Model (A4) > Coordinate Systems > Coordinate System

Object Name	*Global Coordinate System*
State	Fully Defined
Definition	
Type	Cartesian
Coordinate System ID	0.
Origin	
Origin X	0. µm
Origin Y	0. µm
Origin Z	0. µm

Directional Vectors	
X Axis Data	[1. 0. 0.]
Y Axis Data	[0. 1. 0.]
Z Axis Data	[0. 0. 1.]
Transfer Properties	
Source	
Read Only	No

Mesh

TABLE 8
Model (A4) > Mesh

Object Name	*Mesh*
State	Solved
Display	
Display Style	Use Geometry Setting
Defaults	
Physics Preference	Mechanical
Element Order	Program Controlled
Element Size	Default
Sizing	
Use Adaptive Sizing	Yes
Resolution	Default (2)
Mesh Defeaturing	Yes
Defeature Size	Default
Transition	Fast
Span Angle Center	Coarse
Initial Size Seed	Assembly
Bounding Box Diagonal	100.51 µm
Average Surface Area	280.63 µm²
Minimum Edge Length	0.5 µm
Quality	
Check Mesh Quality	Yes, Errors
Error Limits	Aggressive Mechanical
Target Element Quality	Default (5.e-002)
Smoothing	Medium
Mesh Metric	None
Inflation	
Use Automatic Inflation	None
Inflation Option	Smooth Transition
Transition Ratio	0.272
Maximum Layers	5
Growth Rate	1.2
Inflation Algorithm	Pre
Inflation Element Type	Wedges
View Advanced Options	No
Advanced	
Number of CPUs for Parallel Part Meshing	Program Controlled
Straight Sided Elements	No
Rigid Body Behavior	Dimensionally Reduced
Triangle Surface Mesher	Program Controlled
Topology Checking	Yes

Pinch Tolerance	Please Define
Generate Pinch on Refresh	No
Statistics	
Nodes	877
Elements	96
Show Detailed Statistics	No

Static Structural (A5)

TABLE 9
Model (A4) > Analysis

Object Name	*Static Structural (A5)*
State	Solved
Definition	
Physics Type	Structural
Analysis Type	Static Structural
Solver Target	Mechanical APDL
Options	
Environment Temperature	22. °C
Generate Input Only	No

TABLE 10
Model (A4) > Static Structural (A5) > Analysis Settings

Object Name	*Analysis Settings*
State	Fully Defined
Step Controls	
Number Of Steps	1.
Current Step Number	1.
Step End Time	1. s
Auto Time Stepping	Program Controlled
Solver Controls	
Solver Type	Program Controlled
Weak Springs	Off
Solver Pivot Checking	Program Controlled
Large Deflection	Off
Inertia Relief	Off
Quasi-Static Solution	Off
Rotordynamics Controls	
Coriolis Effect	Off
Restart Controls	
Generate Restart Points	Program Controlled
Retain Files After Full Solve	No
Combine Restart Files	Program Controlled
Nonlinear Controls	
Newton-Raphson Option	Program Controlled
Force Convergence	Program Controlled
Moment Convergence	Program Controlled
Displacement Convergence	Program Controlled
Rotation Convergence	Program Controlled
Line Search	Program Controlled
Stabilization	Program Controlled
Advanced	

Inverse Option	No
Contact Split (DMP)	Program Controlled
Output Controls	
Stress	Yes
Back Stress	No
Strain	Yes
Contact Data	Yes
Nonlinear Data	No
Nodal Forces	No
Volume and Energy	Yes
Euler Angles	Yes
General Miscellaneous	No
Contact Miscellaneous	No
Store Results At	All Time Points
Result File Compression	Program Controlled
Analysis Data Management	
Solver Files Directory	C:\Users\Acer\Desktop\gold_files\dp0\SYS\MECH\
Future Analysis	None
Scratch Solver Files Directory	
Save MAPDL db	No
Contact Summary	Program Controlled
Delete Unneeded Files	Yes
Nonlinear Solution	No
Solver Units	Active System
Solver Unit System	μmks

TABLE 11
Model (A4) > Static Structural (A5) > Loads

Object Name	*Fixed Support*	*Force*
State	Fully Defined	
Scope		
Scoping Method	Geometry Selection	
Geometry	1 Face	
Definition		
Type	Fixed Support	Force
Suppressed	No	
Define By		Vector
Applied By		Surface Effect
Magnitude		0.1 μN (ramped)
Direction		Defined

FIGURE 1
Model (A4) > Static Structural (A5) > Force

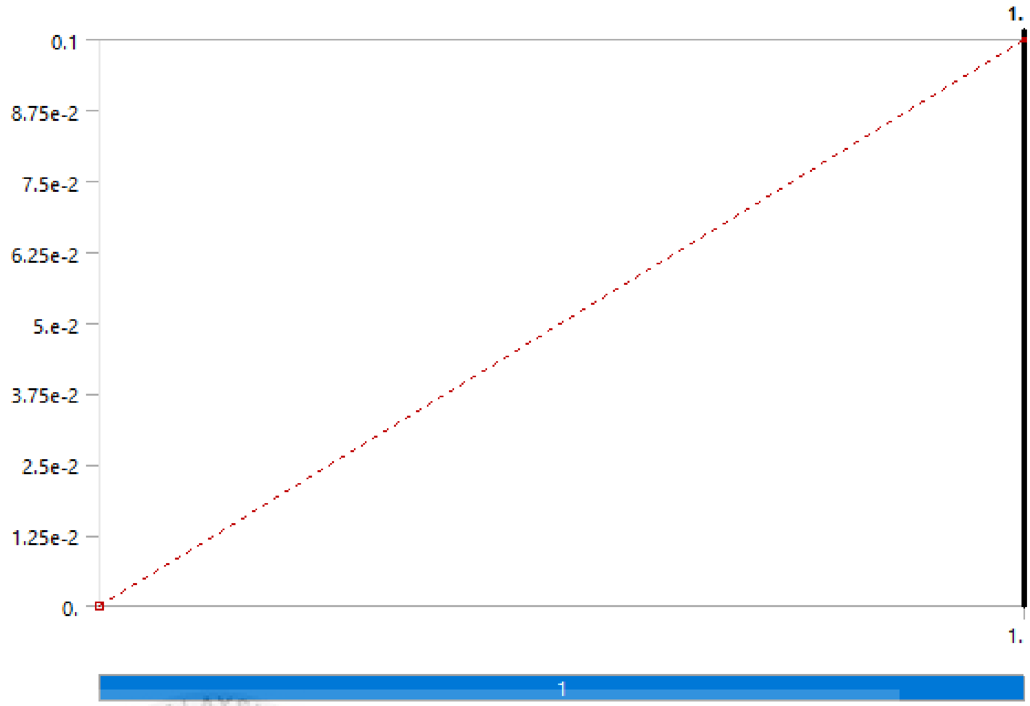

Solution (A6)

TABLE 12
Model (A4) > Static Structural (A5) > Solution

Object Name	*Solution (A6)*
State	Solved
Adaptive Mesh Refinement	
Max Refinement Loops	3.
Refinement Depth	2.
Information	
Status	Done
MAPDL Elapsed Time	3. s
MAPDL Memory Used	181. MB
MAPDL Result File Size	960. KB
Post Processing	
Beam Section Results	No
On Demand Stress/Strain	No

TABLE 13
Model (A4) > Static Structural (A5) > Solution (A6) > Solution Information

Object Name	*Solution Information*
State	Solved
Solution Information	
Solution Output	Solver Output
Newton-Raphson Residuals	0
Identify Element Violations	0
Update Interval	2.5 s
Display Points	All
FE Connection Visibility	

Activate Visibility	Yes
Display	All FE Connectors
Draw Connections Attached To	All Nodes
Line Color	Connection Type
Visible on Results	No
Line Thickness	Single
Display Type	Lines

TABLE 14
Model (A4) > Static Structural (A5) > Solution (A6) > Results

Object Name	*Total Deformation*	*Directional Deformation*	*Equivalent Stress*	*Normal Stress*
State	Solved			
Scope				
Scoping Method	Geometry Selection			
Geometry	All Bodies			
Definition				
Type	Total Deformation	Directional Deformation	Equivalent (von-Mises) Stress	Normal Stress
By	Time			
Display Time	Last			
Separate Data by Entity	No			
Calculate Time History	Yes			
Identifier				
Suppressed	No			
Orientation		X Axis		X Axis
Coordinate System		Global Coordinate System		Global Coordinate System
Results				
Minimum	0. µm	-3.1834e-003 µm	3.2753e-003 MPa	-9.1337 MPa
Maximum	0.43793 µm	6.3503e-003 µm	6.061 MPa	7.6593 MPa
Average	0.1221 µm	2.7609e-004 µm	2.0183 MPa	-3.4065e-002 MPa
Minimum Occurs On	Solid			
Maximum Occurs On	Solid			
Information				
Time	1. s			
Load Step	1			
Substep	1			
Iteration Number	1			
Integration Point Results				
Display Option			Averaged	
Average Across Bodies			No	

FIGURE 2
Model (A4) > Static Structural (A5) > Solution (A6) > Total Deformation

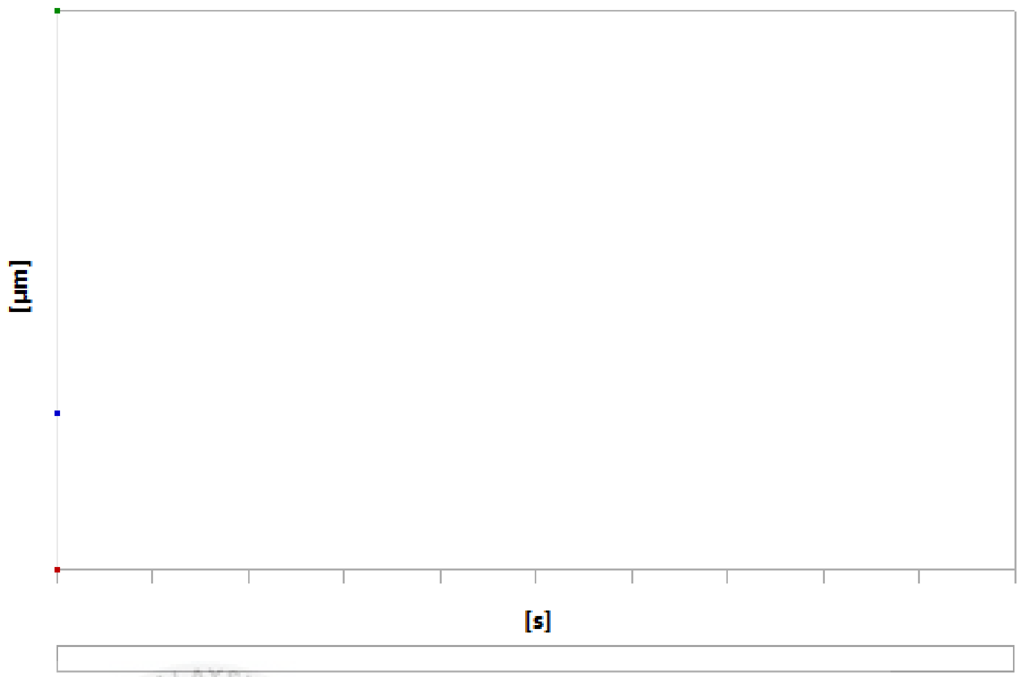

TABLE 15
Model (A4) > Static Structural (A5) > Solution (A6) > Total Deformation

Time [s]	Minimum [µm]	Maximum [µm]	Average [µm]
1.	0.	0.43793	0.1221

TABLE 16
Model (A4) > Static Structural (A5) > Solution (A6) > Total Deformation > Convergences

Object Name	*Convergence*
State	Solved
Definition	
Type	Maximum
Allowable Change	1. %
Results	
Last Change	0.33584 %
Converged	Yes

FIGURE 3
Model (A4) > Static Structural (A5) > Solution (A6) > Total Deformation > Convergence

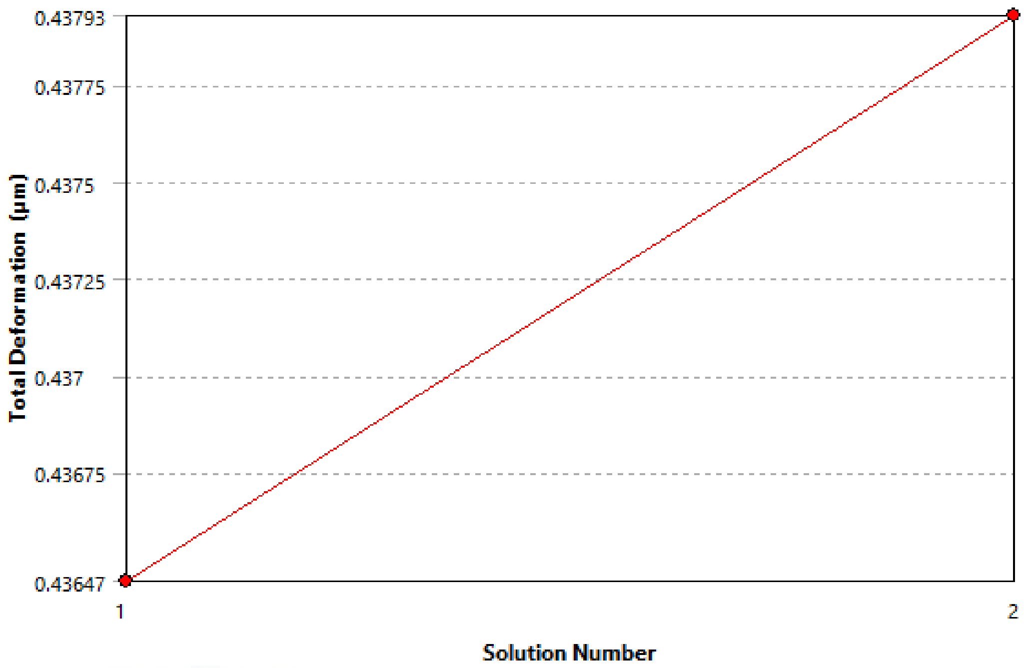

Model (A4) > Static Structural (A5) > Solution (A6) > Total Deformation > Convergence

	Total Deformation (µm)	Change (%)	Nodes	Elements
1	0.43647		877	96
2	0.43793	0.33584	2079	939

FIGURE 4
Model (A4) > Static Structural (A5) > Solution (A6) > Total Deformation > Gold cantilever

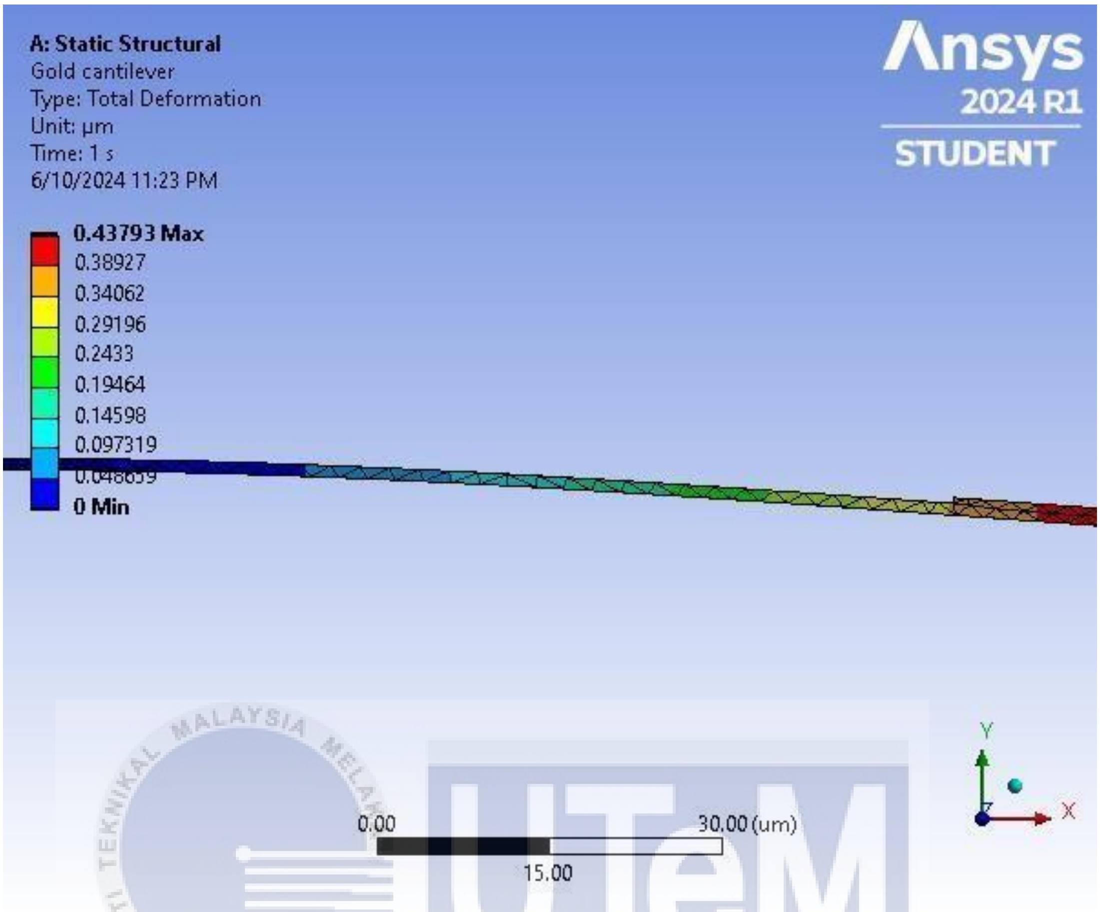

FIGURE 5

Model (A4) > Static Structural (A5) > Solution (A6) > Total Deformation > Gold2

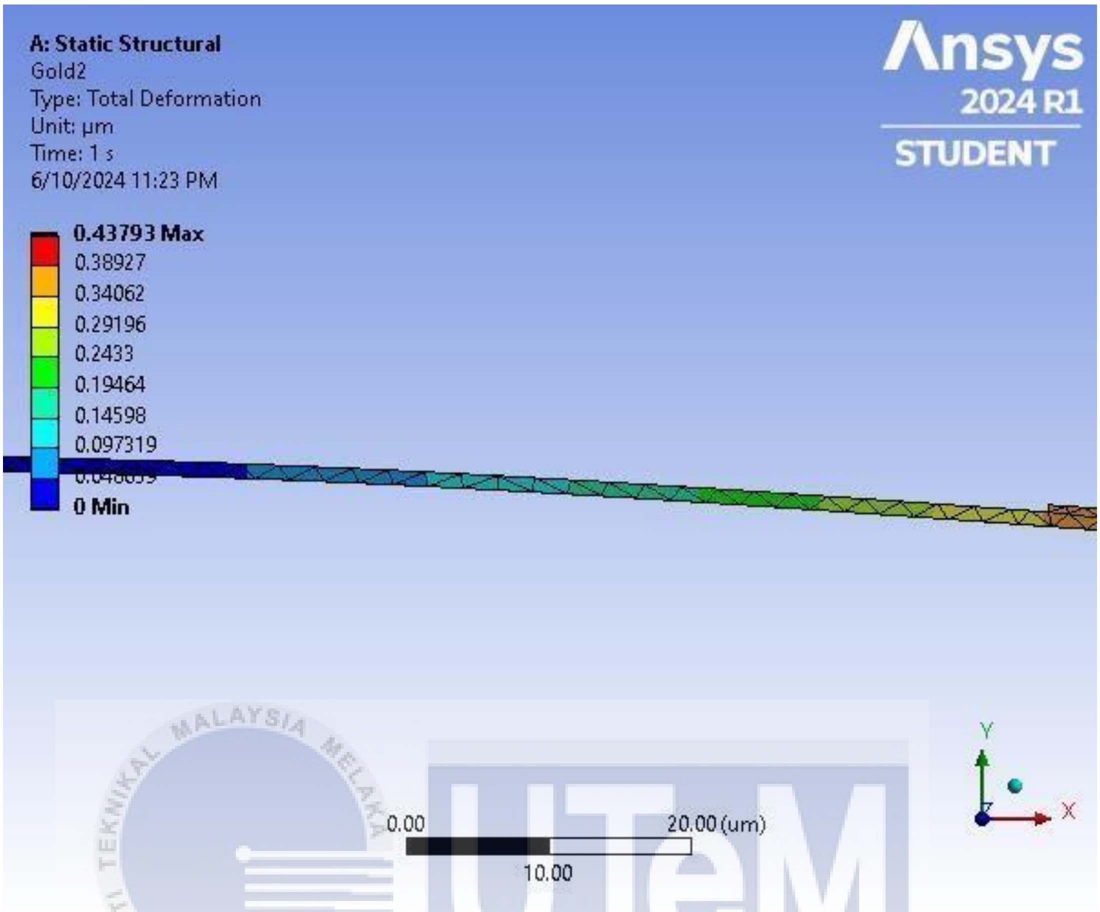

FIGURE 6
Model (A4) > Static Structural (A5) > Solution (A6) > Directional Deformation

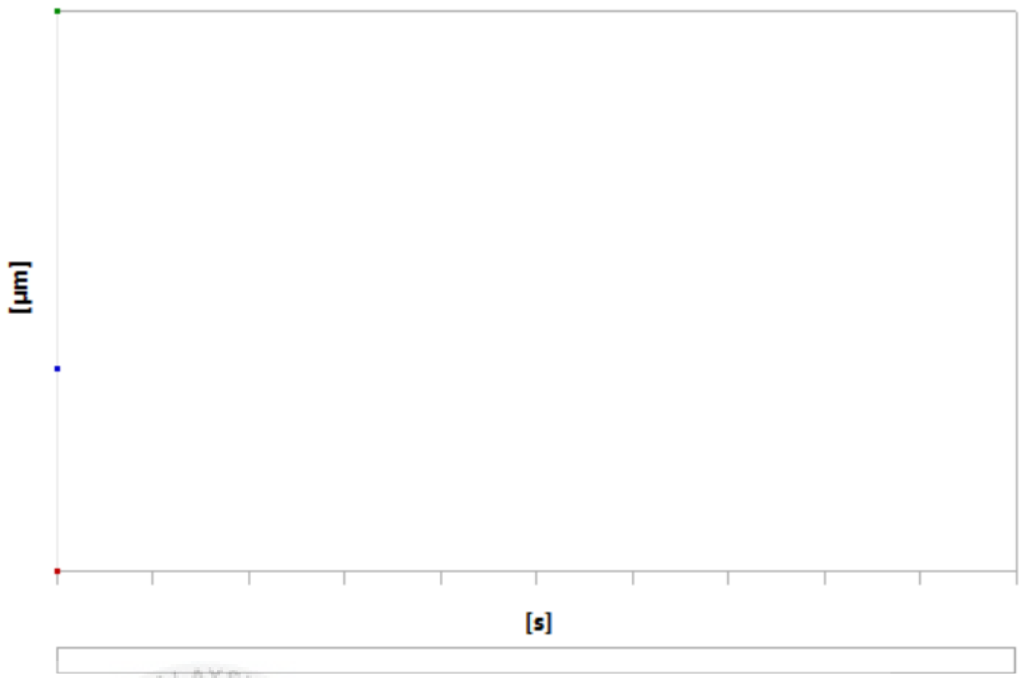

TABLE 17
Model (A4) > Static Structural (A5) > Solution (A6) > Directional Deformation

Time [s]	Minimum [µm]	Maximum [µm]	Average [µm]
1.	-3.1834e-003	6.3503e-003	2.7609e-004

FIGURE 7
Model (A4) > Static Structural (A5) > Solution (A6) > Equivalent Stress

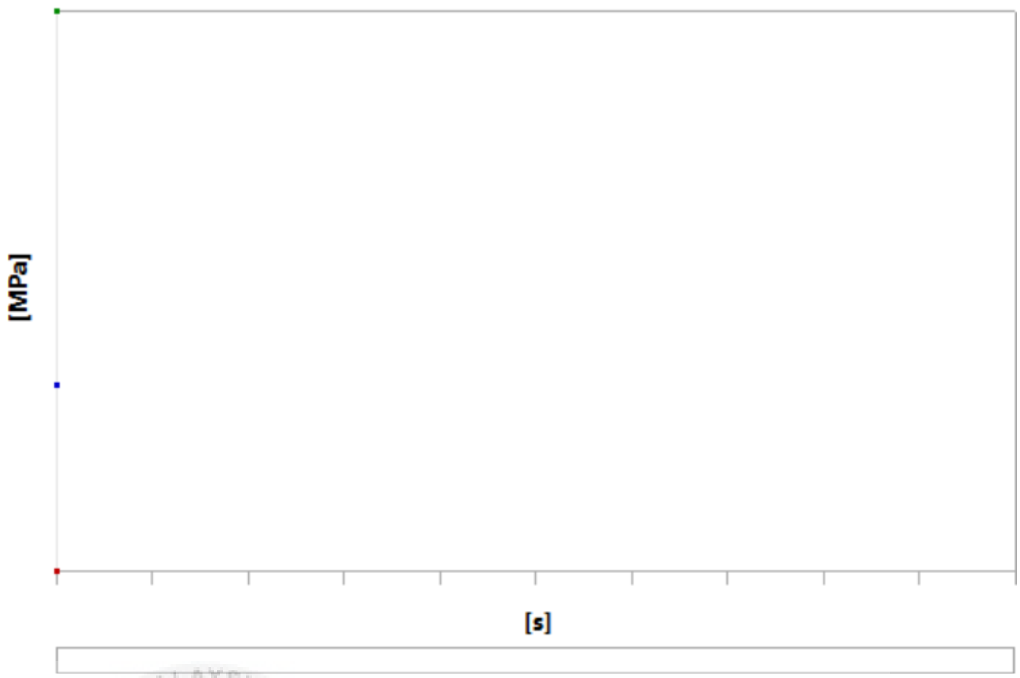

TABLE 18
Model (A4) > Static Structural (A5) > Solution (A6) > Equivalent Stress

Time [s]	Minimum [MPa]	Maximum [MPa]	Average [MPa]
1.	3.2753e-003	6.061	2.0183

FIGURE 8
Model (A4) > Static Structural (A5) > Solution (A6) > Normal Stress

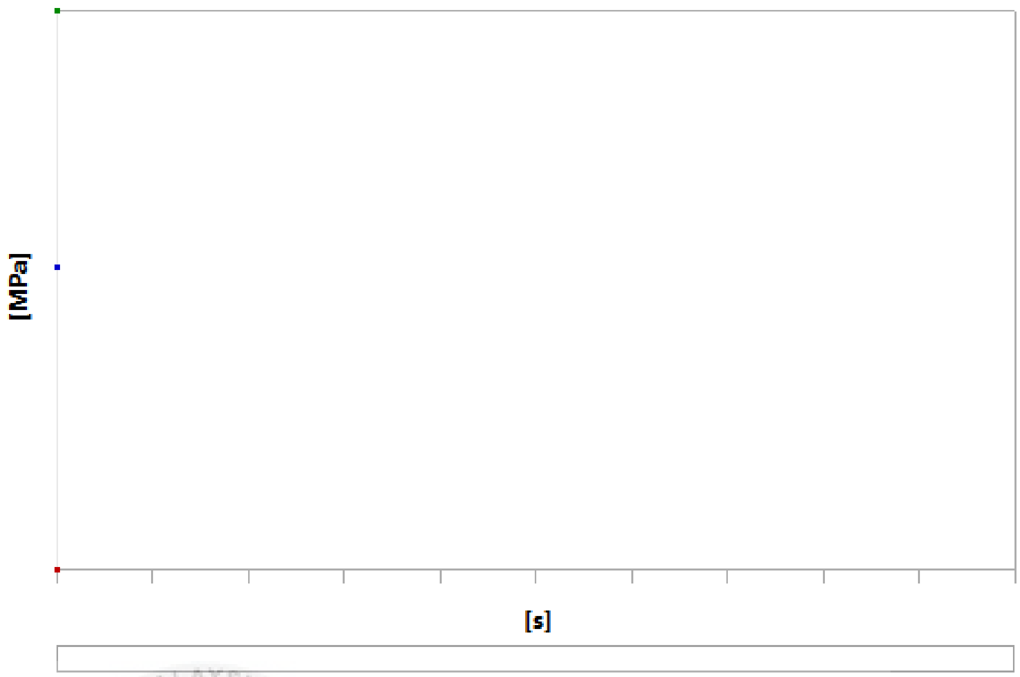

TABLE 19
Model (A4) > Static Structural (A5) > Solution (A6) > Normal Stress

Time [s]	Minimum [MPa]	Maximum [MPa]	Average [MPa]
1.	-9.1337	7.6593	-3.4065e-002

Material Data

Gold

TABLE 20
Gold > Color

Red	Green	Blue
234	247	209

TABLE 21
Gold > Isotropic Elasticity

Young's Modulus MPa	Poisson's Ratio	Bulk Modulus MPa	Shear Modulus MPa	Temperature C
79000	0.42	1.6458e+005	27817	

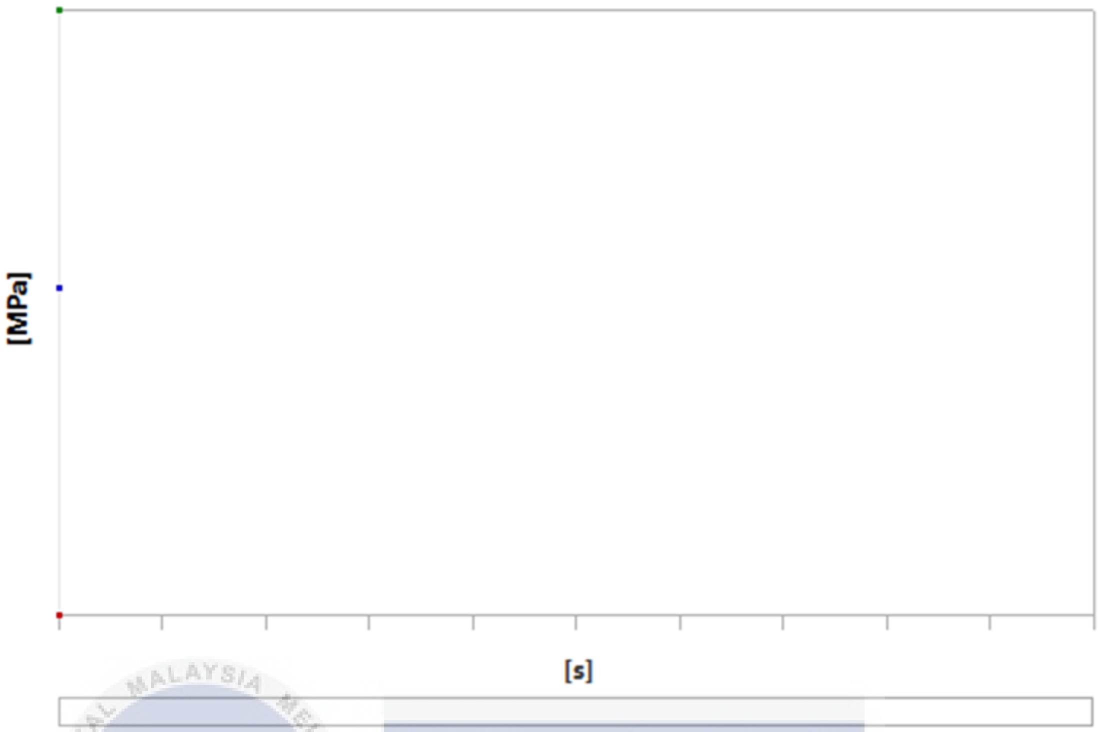
[MPa]
[s]